PHENOTYPICAL CHARACTERIZATION OF MICRORNA-106B OVEREXPRESSION IN MCF10A BREAST CELL LINE

A THESIS SUBMITTED TO
THE GRADUATE SCHOOL OF NATURAL AND APPLIED SCIENCES
OF
MIDDLE EAST TECHNICAL UNIVERSITY

BY

CANSARAN SAYGILI

IN PARTIAL FULFILLMENT OF THE REQUIREMENTS
FOR
THE DEGREE OF MASTER OF SCIENCE
IN
BIOLOGY

FEBRUARY 2013

Approval of the Thesis

PHENOTYPICAL CHARACTERIZATION OF MICRORNA-106B OVEREXPRESSION IN MCF10A BREAST CELL LINE

submitted by **CANSARAN SAYGILI** in partial fulfillment of the requirements for the degree of **Master of Science in Biology Department, Middle East Technical University** by,

Prof. Dr. Canan Özgen _____
Dean, Graduate School of **Natural and Applied Sciences**

Prof. Dr. Gülay Özcengiz _____
Head of Department, **Biology**

Assoc. Prof. Dr. A.Elif Erson-Bensan _____
Supervisor, **Biology Dept., METU**

Examining Committee Members:

Assoc. Prof. Dr. Mesut Muyan _____
Biology Dept., METU

Assoc. Prof. Dr. A.Elif Erson-Bensan _____
Biology Dept., METU

Assoc. Prof. Dr. Mayda Gürsel _____
Biology Dept., METU

Assist. Prof. Dr. Tülin Yanık _____
Biology Dept., METU

Assist. Prof. Dr. Bala Gür-Dedeoğlu _____
Biotechnology Institute, Ankara University

Date: 01.02.2013

I hereby declare that all information in this document has been obtained and presented in accordance with academic rules and ethical conduct. I also declare that, as required by these rules and conduct, I have fully cited and referenced all material and results that are not original to this work.

Name, Last name: Cansaran Saygılı

Signature :

ABSTRACT

PHENOTYPICAL CHARACTERIZATION OF MICRORNA-106B OVEREXPRESSION IN MCF10A BREAST CELL LINE

Saygılı, Cansaran
M.Sc., Department of Biology
Supervisor: Assoc. Prof. Dr. A. Elif Erson-Bensan

February 2013, 74 Pages

MicroRNAs are small non-coding RNAs which regulate gene expression by binding to 3'UTR of their target mRNAs. Deregulated expression of microRNAs is detected in many pathologies including different types of cancers. miR-106b, is a member of miR-106b-25 cluster and overexpressed in many cancers including breast cancer. Based on miR-106b overexpression, we hypothesized that miR-106b may be an oncogene candidate. To explore miR-106b related phenotypes, we used an already miR-106b transfected model cell line system. Stably transfected MCF10A cells were investigated for alterations in cell growth, motility, migration and invasion. Our results showed that miR-106b overexpression caused increased growth motility and migration. On the other hand, based on matrigel invasion assay miR-106b expression caused a reduction in cell invasion. Further studies are needed to be performed to understand the precise role of miR-106b in breast cancer. Studies are underway to detect possible miR-106b targets that may help to explain these phenotypical alterations.

Key Words: Breast cancer, microRNAs, miR-106b

öz

MİKRORNA-106B AŞIRI İFADESİNİN MCF10A MEME HÜCRELERİNDE FENOTİPİK KARAKTERİZASYONU

Saygılı, Cansaran
M.Sc., Biyoloji Bölümü
Tez Yöneticisi: Doç. Dr. A. Elif Erson-Bensan

Şubat 2013, 74 Sayfa

MikroRNA' lar protein kodlamayan küçük RNA molekülleridir. Gen ifadesini genellikle hedef mRNA ların 3' protein kodlamayan bölgelerine bağlanarak kontrol ederler. Kanser de dahil olmak üzere, pek çok hastalıkta mikroRNA'ların ifade seviyesinde düzensizlikler saptanmıştır. miR-106b-25 kümesinin bir üyesi olan miR-106b'nin ifadesinin meme kanseri de dahil olmak üzere pek çok kanser türünde arttığı gösterilmiştir. miR-106b seviyesindeki artışlar göz önüne alınarak, miR-106b olası bir onkogen olarak düşünülmüştür. Bu nedenle, daha önce oluşturulmuş miR-106b transfekte edilmiş bir hücre hattı modeli kullandık. Kalıcı olarak transfekte edilmiş MCF10A hücreleri ; hücre büyümesi, hareketliliği, migrasyonu ve invasyonu açısından incelenmiştir. Elde edilen bulgular, miR-106b ifadesindeki artışın hücre büyümesini, hücrelerin hareketini ve migrasyonunu arttırdığını göstermiştir. Öte yandan, miR-106b'nin invasyonu azalttığı matrigel invasyon deneyleri sonucunda gösterilmiştir. miR-106b'nin meme kanserindeki rolünü tam olarak anlayabilmek için pek çok çalışmanın yapılması gerekmektedir. Gözlemlediğimiz fenotipik değişiklikleri açıklayabilmek için olası miR-106b hedef mRNA dizileri araştırılmakta ve bununla ilgili çalışmalarımız devam etmektedir.

Anahtar Kelimeler: Meme kanseri, mikroRNA, miR-106b

To my mother
Muzaffer Saygılı

ACKNOWLEDGEMENTS

First and foremost, I would like to express my deepest appreciation to my supervisor Assoc. Prof. Dr. A.Elif Erson-Bensan for her endless support, motivation and immense knowledge. Without her inspiring guidance and encouragement, I couldn't have accomplished this thesis successfully.

Besides my supervisor, I would like to thank all my thesis committee members: Assoc.Prof.Dr.Mesut Muyan, Assoc. Prof. Dr. Mayda Gürsel, Assist. Prof. Dr. Tülin Yanık and Assist. Prof. Dr. Bala Gür-Dedeoğlu.

My grateful thanks also extended to Dr. Mesut Muyan for his insightful comments and precious advice. His willingness to give his time so generously has been very much appreciated.

I would like to express my sincere thanks to all previous and current lab members of our lab, Ayşegül Sapmaz, Begüm Akman, Taner Tuncer, Shiva Akhavantabasi, Merve Öyken, Nihan Özdemirler, Gizem Güpür, Neşe Erdem and Serkan Tuna for providing a stimulating and fun filled environment and for their precious friendship. My thanks go in particular to Ayşegül Sapmaz who started this project and helped me a lot during this study. My special appreciation goes to Serkan Tuna who trusted and supported me from the beginning of my undergraduate years. Besides his scientific motivation, I am thankful for his invaluable friendship.

I would like to thank Assoc. Prof. Dr. Sreeparna Banerjee's lab members for sharing their resources throughout this thesis research.

I would like to extend huge, warm thanks to my friends Giray Bulut, Sinem Güven, Pınar Kaya, Gülay Kılıçaslan, Öykü Koçak and Cansın Yavuz for their love, care and moral support. They were always there to cheer me up in all the tough times.

Words fail me to express my appreciation to my mother, Muzaffer Saygılı, for her love, constant support, care and understanding throughout my life. I wouldn't be here without her encouragement. It is to her that I dedicate this work.

Last but not least, I wish to offer my deepest thanks to Mustafa Demir. He was always beside me during the happy and hard moments to push me and motivate me. Without his love, support and endless understanding, this accomplishment wouldn't have been made possible.

I would like to thank TUBITAK for the National Scholarship Programme for Master Students.

TABLE OF CONTENTS

ABSTRACT v
ÖZ vi
ACKNOWLEDGEMENTS viii
TABLE OF CONTENTS ix
LIST OF TABLES xi
LIST OF FIGURES xii
LIST OF ABBREVIATIONS xiv
CHAPTERS
1.INTRODUCTION 1
1.1 microRNAs 1
1.1.1 Biogenesis of microRNAs 1
1.1.2 Different Ways of Gene Regulation by microRNAs 6
1.1.3 microRNAs and cancer 8
1.2 miR-17 family 13
1.2.1 miR-106b-25 cluster 13
1.2.2 miR-106b-25 cluster and cancer 15
1.3 Aim of the Study 16
2.MATERIALS AND METHODS 19
2.1 Mammalian Cell Culture Conditions 19
2.2 Transfection of Mammalian Cells 19
2.3 Expression Analysis of miR-106b 20
2.3.1 RNA Isolation by Trizol Reagent 20
2.3.2 Determination of RNA Quantity and Quality 20
2.3.3 DNase I Treatment 20
2.3.4 cDNA synthesis 21
2.3.4 Reverse Transcription Polymerase Chain Reaction (RT-PCR) 22
2.3.4.1 Densitometry Analysis of RT-PCR 23
2.3.5 Detection of mature miR-106b levels 23
2.3.5.1 Analysis of TaqMan qRT-PCR results 26
2.4 Functional Assays 27
2.4.1 Growth curve analysis 27
2.4.2 Cellular Proliferation Assay 27
2.4.3 *In vitro* Wound Closure Assay 28
2.4.4 Transwell migration assay 28
2.4.5 Matrigel Invasion assay 29
3.RESULTS AND DISCUSSION 31
3.1 Generation of miR-106b overexpressing stable breast cell line 31
3.2 Expression analysis of pre-miR106b in MCF10A-EV and MCF10A-106b cells 31
3.3 Expression of mature miR-106b in MCF10A-EV and MCF10A-106b cells 32
3.4 Functional assays 33
3.4.1 Cellular Proliferation 33
3.4.1.1 Growth curve analysis 33
3.4.1.2 Cellular Proliferation Assay (MTT) 34
3.4.2 Directional Migration Phenotype 35
3.4.3 Transwell migration assay 37

3.4.4 Matrigel Invasion Assay 45
4.CONCLUSION 51
REFERENCES 53
APPENDICES
A.VECTORS..... 65
B.TESTING SUCCESS of DNase TREATMENT 67
C.MIQE GUIDELINES..... 67

LIST OF TABLES

TABLES

Table 1.1. Key microRNAs involved in cancer 12
Table 2.1. DNase I reaction mixture.....21
Table 2.2. Reaction mixture by RevertAid First Strand cDNA synthesis kit and cDNA synthesis protocol. 21
Table 2.3. List of primers used in RT-PCR. 22
Table 2.4. RT-PCR mixture to amplify pre-miR-106b and *GAPDH*. 22
Table 2.5. RT-PCR cycling conditions for *GAPDH* and hsa-miR-106b. 22
Table 2.6. TaqMan cDNA synthesis reaction mixture and protocol. 23
Table 2.7. TaqMan qRT-PCR mixture. 24
Table 2.8. Thermal cycling conditions for TaqMan qRT-PCR. 24
Table C. MIQE Guidelines Checklist for qRT-PCR 67

LIST OF FIGURES

FIGURES

Figure 1.1. Model for the processing of pri-miRNA by Drosha.....2
Figure 1.2. Model for cleavage of pre-miRNA by Dicer. 3
Figure 1.3. pri-miRNA structure. 4
Figure 1.4. microRNA biogenesis.....5
Figure 1.5. Schematic diagram showing differences and similarities between canonical and mirtron miRNA biogenesis. 6
Figure 1.6. miRNA seed sequences and miRNA binding types in human. 7
Figure 1.7. Gene regulation by microRNAs. 8
Figure 1.8. miRNAs as tumor suppressors or oncogenes. 10
Figure 1.9. Schematic representation of genomic locations of miR-17 family members.....13
Figure 1.10. Schematic representation of miR-106b-25 cluster members in the 13th intron of *MCM7* gene 14
Figure 1.11. Precursor structures of miR-106b-25 cluster members. 14
Figure 2.1. First strand cDNA synthesis with looped RT primer and real time PCR with gene specific forward primers and loop specific reverse primer 25
Figure 2.3. Cleavage of MTT to formazan salt 27
Figure 2.4. Illustration of transwell chamber.....28
Figure 3.1. pre-miR-106b expression analysis by RT-PCR in MCF10A-EV and MCF10A-106b cells. 32
Figure 3.2. Mature miR-106b levels in MCF10A-EV and MCF10A-106b cells.33
Figure 3.3. Growth curve for MCF10A-EV and MCF10A-106b cells. 34
Figure 3.4. MTT assay for MCF10A-EV and MCF10A-106b cells.....35
Figure 3.5. Representative wound healing images of MCF10A-106b and MCF10A-EV.....36
Figure 3.6. Distance travelled by MCF10A-106b and MCF10A-EV cells.....37
Figure 3.7. Migration assay for MCF10A-EV and MCF10A-106b cells. 38
Figure 3.8. Migration assay for MCF10A-EV and MCF10A-106b cells in the absence of EGF 39
Figure 3.9. MTT assay of MCF10A-EV and MCF10A-106b cells in the absence of EGF.....41
Figure 3.10. Images of MCF10A-EV and MCF10A-106b cells after 24 hours starvation in medium containing 1% serum 42
Figure 3.11. Predictions for *STAT3* as target of miR-106b 44
Figure 3.12. Predictions for *AKT3* as target of miR-106b. 45
Figure 3.13. Matrigel invasion assay for MCF10A-EV and MCF10A-106b cells. 46
Figure 3.14. Matrigel invasion assay for MDA-MB-231 and MCF10A-EV cells. 47
Figure 3.15. Predictions for *MMP2* as target of miR-106b 48
Figure 3.16. Predictions for *MMP24* as target of miR-106b. 49
Figure A. Map of pSUPER.retro.neo+GFP (Invitrogen). 65
Figure B. Lack of DNA contamination in RNA samples after DNase treatment 66
Figure C1. RNA concentrations (A_{260}) of MCF10A-EV and MCF10A-106b. 70

Figure C2. qRT-PCR assay performance shown with respect to MIQE guidelines.. 71
Figure C3. qRT-PCR assay performance shown with respect to MIQE guidelines. 73

LIST OF ABBREVIATIONS

Bp	Base pairs
cDNA	Complementary Deoxyribonucleic Acid
DNA	Deoxyribonucleic Acid
DNase I	Deoxyribonuclease I
dNTP	Deoxyribonucleotide triphosphate
G	Centrifuge gravity force
miRNA	microRNA
mRNA	messenger RNA
PCR	Polymerase chain reaction
Pri-miRNA	Primary microRNA
Pre-miRNA	Precursor microRNA
qRT-PCR	Quantitative Real Time Polymerase Chain Reaction
RISC	RNA-induced Silencing Complex
RNA	Ribonucleic acid
RNase	Ribonuclease
RT-PCR	Reverse Transcription Polymerase Chain Reaction
UTR	Untranslated Region

CHAPTER 1

INTRODUCTION

1.1 microRNAs

microRNAs (miRNAs) were discovered in 1993 in a study focusing on developmental timing in *Caenorhabditis elegans* [1]. Following this study, microRNAs were discovered in other organisms such as *Drosophila melanogaster* [2], mammals [3], plants [4] and viruses [5]. miRBase (a database for microRNAs) Release 19 , as of August 2012, contains 21264 entries representing hairpin precursor miRNAs, expressing 25141 mature miRNA products, in 193 species [6] (http://www.mirbase.org/). For *Homo sapiens* 1600 precursor and 2042 mature microRNA sequences have been submitted to miRBase.

Based on a study conducted on plant miRNAs, miRNAs were predicted to be at least 400 million years old [7]. Being evolutionarily ancient and conserved among different species, a maintained role for miRNAs throughout evolution might be suggested.

1.1.1 Biogenesis of microRNAs

miRNAs are 19-22 nucleotide long, single stranded RNAs that play roles in gene regulation [8]. Most miRNAs are transcribed by RNA polymerase II (Pol II) into primary miRNA transcripts (pri-miRNA) [9]. The specific feature of RNA Pol II transcribed miRNAs is the presence of 3' poly A tail and 5' cap. The length of pri-miRNA transcript varies from several hundred to several kilobases [10]. Small proportion of miRNAs -that are found in downstream of Alu elements- are thought to be transcribed by RNA polymerase III (Pol III) [11]. Conversely, the miRNAs that were found to be associated with RNA polymerase III in the previous study [11] , was not confirmed in another study [12]. Instead two other microRNA genes, miR-886 and miR-1975, were suggested as RNA Pol III transcribed microRNAs [12].

Stem-loop structure of pri-miRNAs is processed in nucleus to form precursor hairpin miRNA (pre-miRNA) by endonucleolytic cleavage of nuclear microprocessor complex [13]. This complex is formed from RNase III enzyme (Drosha) and DGCR8 (DiGeorge critical region 8) protein (also known as Pasha (Partner of Drosha) in *D. melanogaster* and *C. elegans*) [14,15,16]. DGCR8/Pasha is a 120 kDa protein and contains two double stranded RNA binding domains [16,17]. Drosha is a 160 kDa protein and contains two tandem RNase III domains (RIIIDs) which are critical for catalysis [18]. A regular human pri-miRNA has a hairpin stem of 33 base-pairs, a terminal loop and

two single stranded flanking regions (at upstream and downstream of flanking regions). Flanking regions and hairpin stem are critical for DGCR8 binding and Drosha cleavage [19]. DGCR8 stably interacts with pri-miRNA and behaves as a ruler to determine the exact cleavage site. Next; Drosha, an RNase, cleaves at a site 11 base pair away from the single-stranded-double stranded RNA junction. Hence, Drosha processing results with a 2 nucleotide overhang at the 3'end of pre-miRNA and this overhang is required for successful export from nucleus [20] (Figure 1.1).

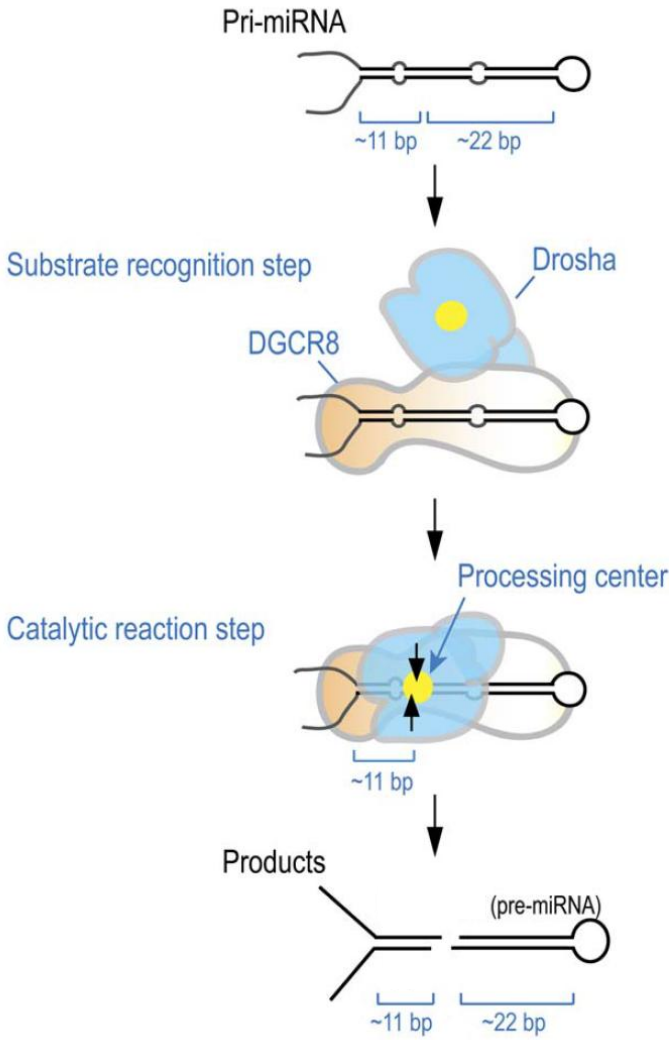

Figure 1.1. Model for the processing of pri-miRNA by Drosha. 33 bp stem of pri-miRNA contains two parts designated as lower (11 bp) and upper (22 bp) stems. DGCR8 recognizes the pri-miRNA substrate from ssRNA-dsRNA junction. After the recognition step, Drosha interacts with substrate for catalysis. The processing center (yellow circle) of Drosha is positioned at ~11 bp from the basal segment. Cleavage results in pre-miRNA with a 2 nucleotide overhang at the 3' end (Taken from [20]).

Export of pre-miRNA into the cytoplasm is performed by Exportin-5 in complex with Ran-GTP [21]. Once pre-miRNA is in the cytoplasm, it is exposed to the second processing step by Dicer (RNase III enzyme in cytoplasm) to form a ~22 nt long mature microRNA [22,23]. Dicer is a multi-domain protein which contains the N-terminal DEAD-box helicase domain -responsible for separation of double-stranded duplex- , the Piwi-Argonaute-Zwille (PAZ) domain -binds to 3' flanking end in pre-miRNAs- , two RNase III domains (RIIIA and RIIIB) and the C-terminal dsRNA binding domain (dsRBD) [17,24] (Figure 1.2).

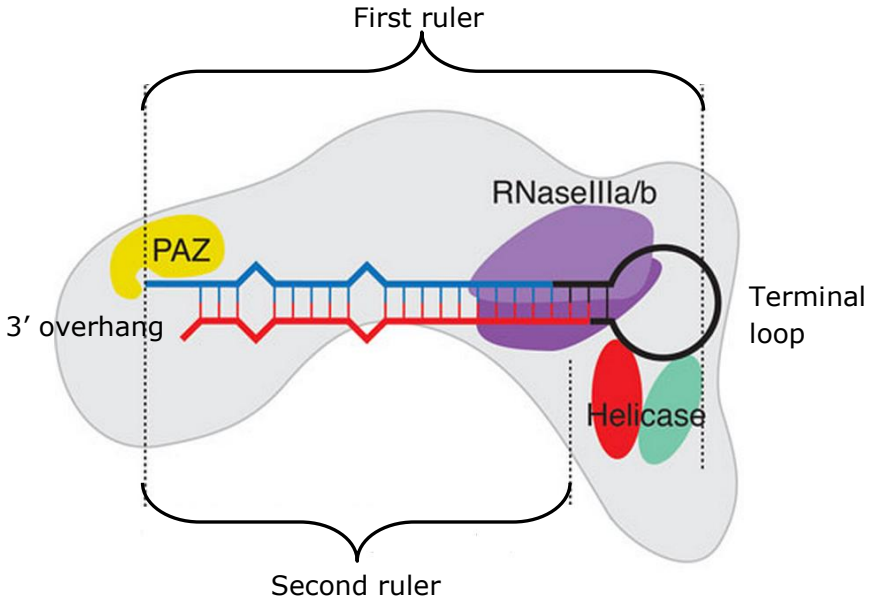

Figure 1.2. Model for cleavage of pre-miRNA by Dicer. Via its PAZ (Piwi-Argonaute-Zwille) and helicase domains, Dicer checks the distance from 3' overhang to the terminal loop of pre-miRNA (First ruler). Then, via its RNase III domains cut the pre-miRNA at a fixed distance 22 nt (second ruler) from the 3'overhang (Taken from [25]).

Structure of pri-miRNA and cleavages sites for Drosha and Dicer are shown in Figure 1.3.

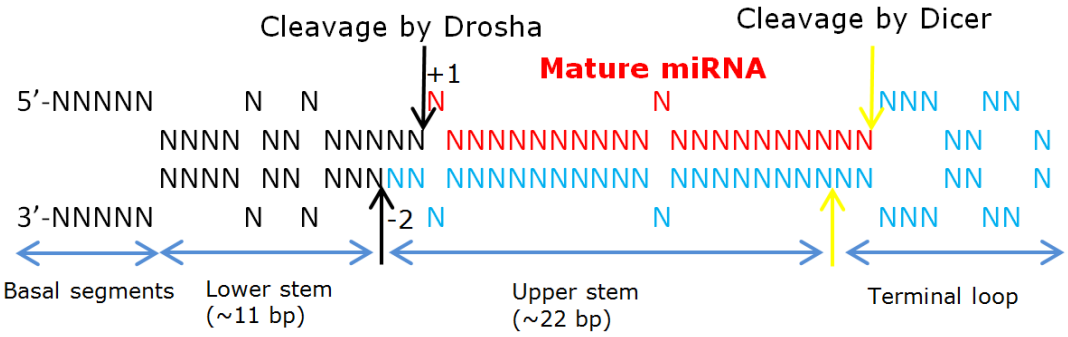

Figure 1.3. pri-miRNA structure. A pri-miRNA can be divided into four parts: basal segments, lower stem, upper stem and a terminal loop. Cleavage sites of Drosha and Dicer are indicated with black and yellow arrows, respectively (Taken from [20]).

After formation of ~22 nt long mature miRNA duplex intermediate, this complex is loaded into a multi-protein complex named as RNA-induced silencing complex (RISC). RISC is composed of Dicer, TRBP (human immunodeficiency virus-1 trans-activating responsive element (TAR) RNA-binding protein), and Argonaute2 (Ago2) proteins [26]. In theory, the miRNA-duplex could give rise to two different mature miRNAs, though only one miRNA strand (guide strand) is usually incorporated into RISC, whereas the other strand (passenger strand or miRNA*) is degraded [27]. In the miRNA strand selection process, thermodynamic stability of the strands is thought to play an important role [28]. In some rare cases both miRNA and miRNA* may be functional and may target different mRNAs in a tissue dependent manner [29]. Biogenesis of microRNAs is summarized in Figure 1.4.

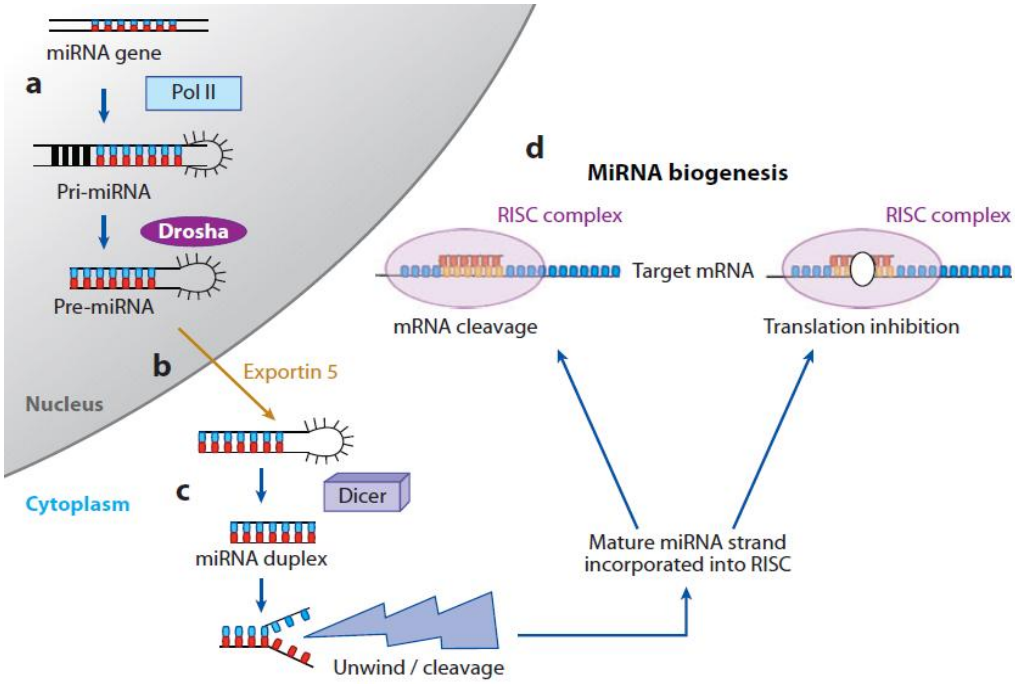

Figure 1.4. microRNA biogenesis. microRNAs are transcribed by RNA polymerase II into pri-miRNA transcripts, then recognized by Drosha and cleaved into pre-miRNA (a). pre-miRNA is transported into the cytoplasm by exportin 5 (b). In the cytoplasm pre-miRNA is processed by Dicer into mature miRNA and only one strand of mature miRNA is incorporated into RISC (c). Depending on complementarity between miRNA and target , mRNA is cleaved or translation is inhibited (d) (Taken from [30]).

A non-canonical pathway for microRNA biogenesis was also described in *Drosophila melanogaster* [31] and *Caenorhabditis elegans* [32]. This pathway is called the "mirtron" pathway. Mirtron loci (short introns which have hairpin potential) give rise directly to pre-miRNA hairpin mimics which circumvent Drosha cleavage. After splicing and debranching, mirtrons can join the canonical pathway at nuclear export stage and then get cleaved by Dicer and form the miRNA/miRNA* duplexes [33] (Figure 1.5). Number of evidence for mammalian mirtrons is also increasing [34,35].

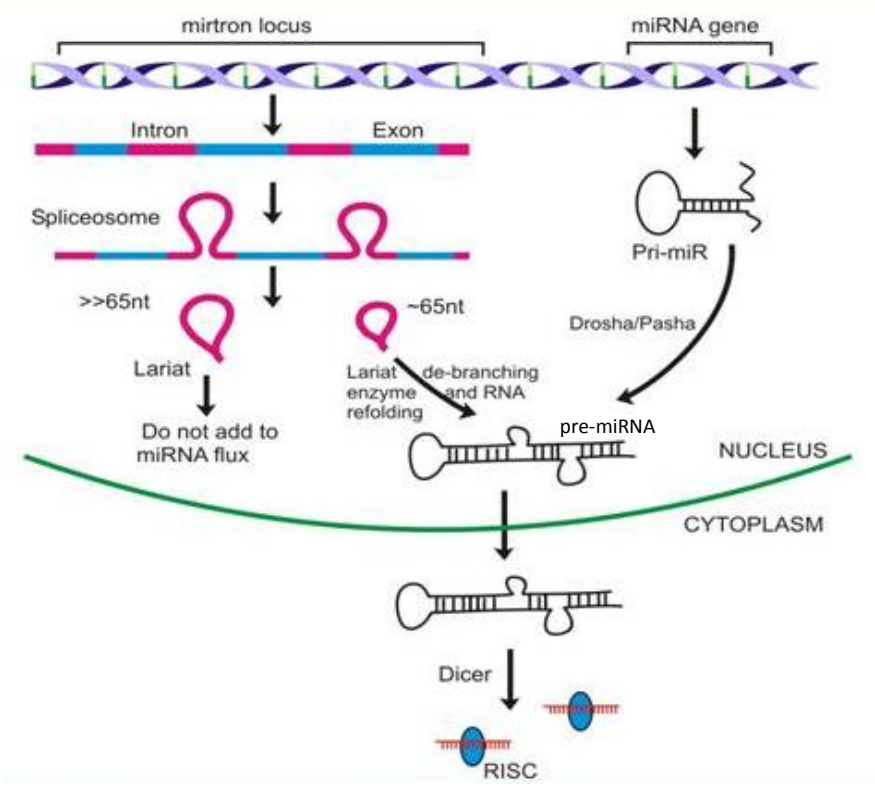

Figure 1.5. Schematic diagram showing differences and similarities between canonical and mirtron miRNA biogenesis. Canonical miRNA biogenesis pathway: Drosha/Pasha (or DGCR8 in vertebrates) cleavage forms pre-miRNA. Mirtron pathway: Introns are spliced and lariats are formed. Lariats that are ~65 nt in length are debranched by lariat debranching enzyme and pre-miRNA is formed. Lariats that are longer than 65 nt are not added to miRNA flux. After pre-miRNA is transported to the cytoplasm, it is processed by Dicer and mature miRNA is formed and loaded onto RISC (Taken from [36]).

1.1.2 Different Ways of Gene Regulation by microRNAs

Almost 60% of human protein coding genes are thought to be regulated by miRNAs [37]. Common mechanism in gene regulation by miRNAs is post-transcriptional regulation of gene expression [38]. miRNAs exert their effect by usually binding to 3' untranslated region (UTR) of mRNAs [39] and in some cases miRNAs are found to bind 5'UTR [40,41] or coding regions of their targets [42]. Post-transcriptional regulation can occur by two different mechanisms: mRNA degradation or translational repression [8,42]. Perfect binding of miRNAs to targets result in mRNA cleavage, in plants [43,44]. On the other hand, few studies showed perfect binding of miRNAs to targets in animals as well, which causes mRNA degradation [45,46]. Translational repression; on the other hand, is commonly observed in animals and occurs via imperfect binding of miRNA to target mRNA 3' UTR [47].

Imperfect binding of miRNAs to their targets is feature of animal miRNAs. Although it is stated as 'imperfect', there is a highly conserved region of perfect match between miRNA and mRNA target termed as 'seed region'. Seed region starts from the 2nd nucleotide of the miRNA. Length of this seed region varies between 6 to 8 nucleotides. Although repression efficiency of miRNAs is dependent on some features of 3' UTR (such as nucleotide composition and position of target region in 3' UTR sequence), usually the efficacy is highest in 8-mer and lowest in 6-mer sites [48,49] (Figure 1.6).

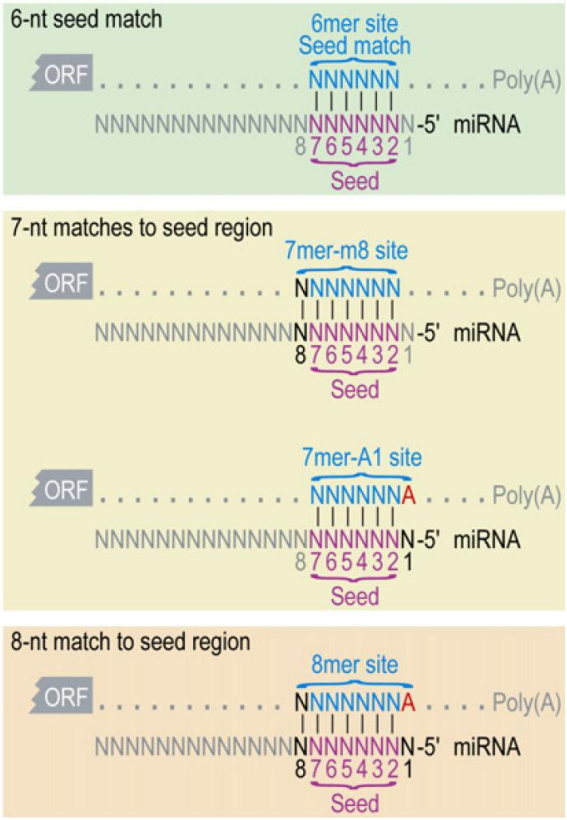

Figure 1.6. miRNA seed sequences and miRNA binding types in human. ORF: Open Reading Frame. 7mer-m8 contains the seed match enhanced by a match to miRNA nucleotide 8. 7mer-A1 contains the seed match enhanced by an A at target position 1 (Taken from [48]).

Due to the short length of seed sequence, a single miRNA can potentially target several mRNAs. For this reason *in silico* methods are used to predict miRNA targets. TargetScan [37,48,50,51], PITA [52], PicTar [53], FindTar3 [54,55] are most commonly used target prediction tools.

In addition to post-transcriptional gene regulation, miRNAs can exert their effect at transcriptional level. They can modulate gene expression by directly

inducing epigenetic modifications of target gene promoters [56]. Transcriptional gene silencing by miRNAs was reported in yeast, plants, mammals [57,58] and in human [59], through *de novo* DNA methylation or chromatin modification. For instance, *HOXD4* expression in breast cancer was found to be inhibited transcriptionally by miRNA-10a. This inhibition was achieved by DNA methylation of HOXD4 promoter [59]. Different effects of miRNA on gene regulation are summarized in Figure 1.7.

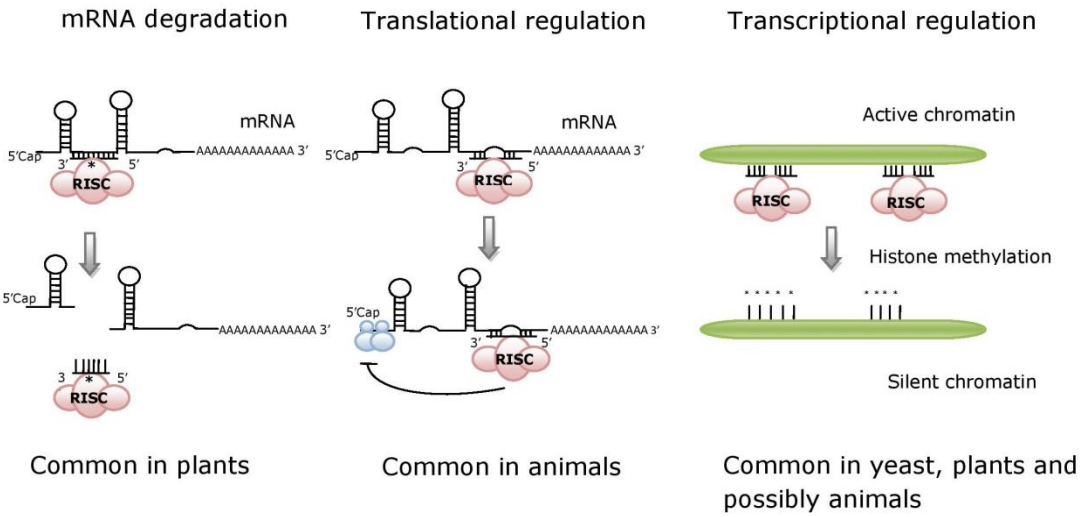

Figure 1.7. Gene regulation by microRNAs. Post-transcriptional regulations can be in two different ways; mRNA degradation or translational inhibition. mRNA degradation is commonly observed in plants with perfect binding of miRNA to target mRNA. Translational regulation is mostly seen in animals in which translation of mRNA is inhibited by binding of miRNA to its target mRNA. In transcriptional regulation, miRNA binding recruits histone methyltransferases (HMT) which methylates histones and cause inhibition of transcription (Adapted from [57]).

1.1.3 microRNAs and cancer

The first data linking miRNAs and cancer was published in 2002 [60]. miR-15 and miR-16 are located on a region (13q14) that is lost in more than half of B cell chronic lymphocytic leukemias (B-CLL). Detailed deletion and expression analysis indicated that both miR-15 and miR-16 is deleted or down-regulated in 68% of CLL cases. In further studies, anti-apoptotic gene *BCL2* was shown as target for these miRNAs [61].

In following studies 186 miRNA genes have been mapped to genomic instability regions. Out of the 186 miRNA genes, 98 of them (52.5%) were found to be located on fragile sites that are associated with cancer [62]. In more recent studies, number of identified miRNAs increased and out of 715

miRNA genes 242 miRNA genes (33.8%) were found to be located on cancer related chromosome fragile sites. Moreover, from those 715 genes 317 of them were positioned within genes that are translocated in cancer [63].

After these studies, indicating involvement of miRNAs in tumorigenesis, many sophisticated tools have been developed to compare miRNA profiles of normal and cancer cells [64]. Commercial miRNA microarrays, bead-based flow cytometry miRNA analysis [65] and high-throughput deep sequencing enabled development of miRNA profiles for normal vs cancer cells [66]. These high-throughput methods showed the striking difference in miRNA profiles of cancer and normal tissue. Moreover, with these methods different subtypes of cancers can even be discriminated based on miRNA profiles [67,68].

Complexity of gene regulation by miRNAs increases with the fact that a single miRNA can target more than one mRNA (as many as 200 targets) and a single mRNA can be regulated by more than one miRNA [53,69]. By regulating a diverse set of genes, miRNAs may potentially affect various aspects of cancer cells; such as self-sufficiency in growth signals, evasion from apoptosis, insensitivity to anti-growth signals [70]. Therefore, miRNA deregulation can contribute to tumorigenesis in several ways.

miRNA expression can be deregulated due to different reasons. Genomic abnormalities (amplification, deletion, translocation, etc.) may cause changes in miRNA expression. In addition to genomic abnormalities, deregulated miRNA expression can result from epigenetic changes. It was shown that half of the genomic sequences of miRNA genes are concomitant with CpG islands [71]. Moreover, some miRNAs were shown to be up-regulated upon exposure of cells to the demethylating agent 5-aza-2'-deoxycytidine [72], upon mutation of DNMTs (DNA methyltransferases) [73] or upon HDAC (histone deacetylase) inhibitor treatment [74]. Another important epigenetic alteration that causes deregulated miRNA expression is hypermethylation of promoters. miR-127, for example, was shown to be silenced in bladder cancer cell lines and patients by promoter hypermethylation [75].

Another factor that affects miRNA expression is transcriptional regulators of miRNAs. Two well-known examples to this regulation are related with *TP53* and *MYC.* TP53 induces the expression of the tumor suppressor miR-34 cluster [76,77], whereas MYC transactivates miR-17-92 cluster [78].

Owing to alterations in miRNA expression, levels of potential mRNA targets will vary under different physiological states of a cell. Like a protein-coding gene, miRNAs can act as tumor suppressors or oncogenes [30] (Figure 1.8).

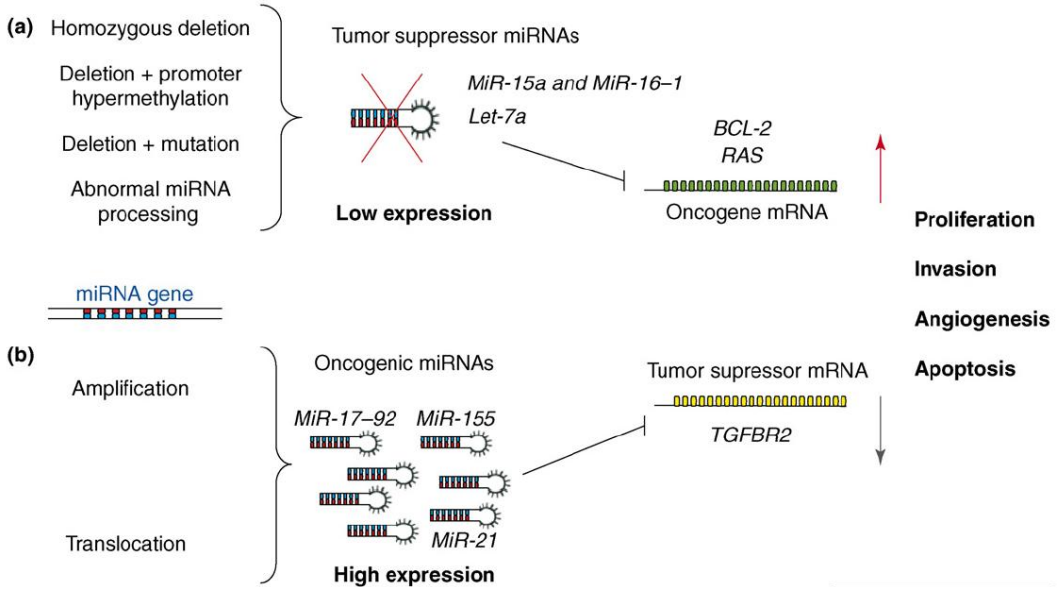

Figure 1.8. miRNAs as tumor suppressors or oncogenes. **a.** miRNAs that down regulate the expression of an oncogene are defined as tumor suppressor miRNAs and are frequently lost in cancer by mutations, deletions, promoter hypermethylation or any abnormalities in miRNA biogenesis. miR-15a, miR-16-1 and let-7a are some examples for tumor suppressor miRNAs. Those tumor suppressor miRNAs target oncogenic mRNAs such as *BCL-2* and *RAS*. Low expression of tumor suppressor miRNAs result in activation of certain pathways related with proliferation, invasion, angiogenesis and apoptosis. **b.** microRNAs that downregulate a tumor suppressor are called oncogenic microRNAs (oncomirs) and they are highly expressed in tumors by amplification or translocation. miR-17-92, miR-155, miR-21 are shown as examples of oncogenic miRNAs. Those oncogenic miRNAs target tumor suppressor mRNAs such as *TGFBR2*. High expression of oncomirs result in activation of certain pathways related with proliferation, invasion, angiogenesis and apoptosis. (Taken from [79]).

Similar to the miR-15 and miR-16 case in CLL [60], let-7 family of miRNAs were down regulated in many cancers such as lung and breast cancer [80,81]. let-7 family members act as tumor suppressors and inhibit well known oncogenes such as *RAS* family [82]. Another tumor suppressor miRNA is miR-125b, aberrant expression of which was shown in many cancers mostly in breast cancer [81,83,84].

One of the first described oncogenic miRNA was miR-155 [85]. Overexpression of miR-155 was shown by many groups in different types of cancers: pediatric Burkitt lymphoma [85], chronic lymphocytic leukemia (CLL) [86], acute myeloid leukemia (AML) [87], lung [80] and breast cancer [81]. In a recent study, *ZNF652* (a zinc finger transcription factor) was identified as a novel target of miR-155. *ZNF652* shows a tumor suppressor role by repressing key proteins of invasion and metastasis [88]. There are several studies showing the oncogenic role of

miR-21 in both hematological malignancies and solid tumors; AML [87], CLL [86], glioblastoma [89], prostate, colon, stomach, lung and breast cancers [90]. Some confirmed targets of miR-21 are *PTEN* (phosphatase and tensin homolog) [91], *PDCD4* (programmed cell death 4) [92], and *TPM1* (tropomyosin 1) [93]. Those proteins have tumor suppressor roles and decreased expression of them by miR-21 causes a tumorigenic phenotype.

The miR-17-92 cluster is a well-studied microRNA family in various types of cancer. Members of this cluster was found to be overexpressed in a variety of cancers; breast, colon, lung, stomach, prostate, pancreas and different types of lymphomas [90,94]. This cluster promotes proliferation mainly by regulating E2F transcription factor which has critical role in cell cycle progression [95]. In contrast, it was reported that this cluster can also act as a tumor suppressor in some cases. Zhang and his colleagues showed deletion of miR-17-92 cluster in 16.5% of ovarian cancers, 21.9% of breast cancers, and 20.0% of melanomas [96]. These data depicted a dual role for miR-17-92 cluster; both as an oncogene and a tumor suppressor.

List of oncogenic and tumor suppressor microRNAs in cancer are summarized in Table 1.1.

Table 1.1. Key microRNAs involved in cancer (Adapted from [30]).

microRNA	Function	Targets	Cancer Type	Reference
miR-15a and miR-16-1	Tumor suppressor	*BCL2* *WT1*	Chronic lymphocytic leukemia (CLL), prostate cancer	60, 61, 97, 98
miR-17-92 cluster	Oncogene	*E2F1*, *BCL2L11*(Bim), *PTEN*, *CDKN1A*(p21)	Lymphomas, breast, lung, colon, stomach, pancreas cancers	90, 99, 94
let-7 (a,-b,-c,-d)	Tumor suppressor	*RASA1*, *MYC*, *HMGA2*	Lung and breast cancer	80, 81, 82, 100
miR-29 (a,-b,-c)	Tumor suppressor	*TCL1*, *MCL1*, *DNMT3*	CLL, Acute myoblastic leukemia (AML), lung and breast cancers, cholangiocarcinoma	86, 80, 81, 101, 102
miR-21	Oncogene	*PTEN, PDCD4, TPM1*	breast, colon, pancreas, lung, prostate, liver, and stomach cancer, AML, CLL and glioblastoma	90, 86, 91, 92
miR-372/ miR-373	Oncogene	*LATS2*	Testicular tumors	103
miR-34a-b-c	Tumor suppressor	*CDK4, CDK6*, *CCNE1*(Cyclin E1), *E2F3*	pancreatic, colon and breast cancers	104,76
miR-155	Oncogene	*MAF*	CLL, AML, Burkitt's lymphoma, lung and breast cancers	90, 80, 81, 105, 106
miR-10b	Tumor suppressor	*HOXD10*	Breast cancer	107
miR-106b-25 cluster	Oncogene	*CDKN1A*, *E2F1*, *BCL2L11*(Bim), *TGFB*, *PTEN, SMAD7*	gastric, colon, and prostate cancer, neuroblastoma, multiple myeloma	108,109,110,111,112

1.2 miR-17 family

According to mature sequence similarities, miRNAs can be grouped into families. miR-17 family is composed of three paralogous polycistronic miRNA clusters which are located on different chromosomes: miR-17~92 (miR-17, miR-18a, miR-19a, miR-20a, miR-19b-1, and miR-92a-1), miR-106b~25 (miR-106b, miR-93, and miR-25), and miR-106a~363 (miR-106a, miR-18b,miR-20b, miR-19b-2, miR-92a-2, and miR-363). During early vertebrate evolution these clusters evolved via several deletion and duplication events [113]. Locations of these paralogous miRNA clusters are depicted in Figure 1.9.

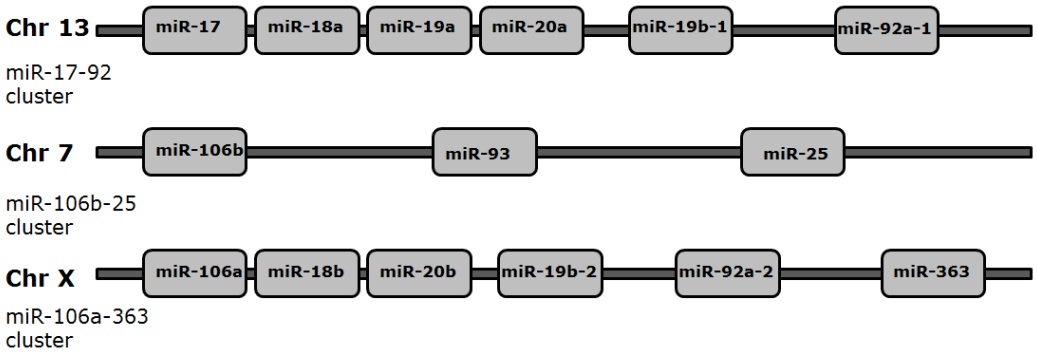

Figure 1.9. Schematic representation of genomic locations of miR-17 family members (Adapted from [110]).

miR-17-92 cluster is the first cluster that was shown to have oncogenic effect [114]. Research to investigate possible roles of miR-106b-25 and miR106a-363 clusters on cancer is continuing.

1.2.1 miR-106b-25 cluster

miR-106b-25 cluster is highly conserved in vertebrates [113]. This cluster harbors three miRNAs; miR-106b, miR-93 and miR-25. All of the members of miR-106b-25 cluster reside in 13th intron of minichromosome maintenance complex component 7 (*MCM7*) gene (Figure 1.10).

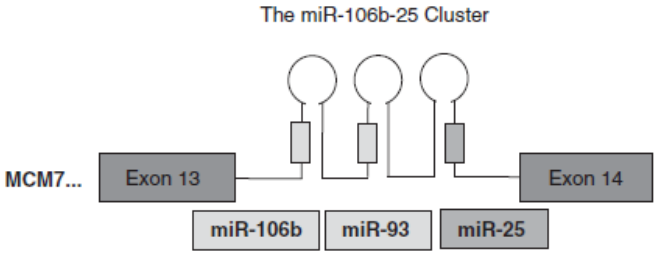

Figure 1.10. Schematic representation of miR-106b-25 cluster members in the 13th intron of *MCM7* gene (Taken from [112]).

Members of this cluster are co-transcribed with the *MCM7* transcript and transcription is regulated similar to that of *MCM7* gene by E2F1 transcription factors [115].

Both precursor and mature sequences of these miRNAs differ from each other. Seed sequences of miR-106b and miR-93 are identical, so they have the potential to target the same mRNAs (Figure 1.11).

A

```
     c      -ua        g        a a     --  uc
ccugc ggggc    aagugcu acagugc g uagu   gg  c
|||||  |||||    |||||||  |||||||  |  ||||  ||
ggacg ccucg    uucaugg ugucacg c aucg   cc  u
     a      ucg        g        c -     ug  uc
```

B

```
          -ca        -      u     g    ug  au
cuggggcuc    aagugcu guucg gcag uag   ug  u
||||||||||    |||||||  |||||  ||||  |||  ||
ggccccgag    uucacga cgagu cguc auc   ac  a
          ccc        u      -     -    ca  cc
```

C

```
     a ug    ag     g      uu g      u    --  ac
ggcc g  uug   aggc gagac   g gcaau gcu   gg  g
||||  |  |||   ||||  |||||   |  |||||  |||  ||  c
ccgg c  gac   ucug cucug   c cguua cgg   cc  u
     c gu    ag     g      uu a      -    gu  cg
```

Figure 1.11. Precursor structures of miR-106b-25 cluster members. Nucleotides in red indicate mature miRNA sequences. **A.** pre-miR-106b hairpin structure. **B.** pre-miR-93 hairpin structure. **C.** pre-miR-25 hairpin structure. Same seed sequences of miR-106b and miR-93 are underlined.

1.2.2 miR-106b-25 cluster and cancer

Deregulated expression of members of miR-106b-25 cluster has been shown in different types of cancers. Using 20 gastric primary tumors and 6 gastric cancer cell lines Petrocca et al. performed a miRNA microarray and identified deregulated miRNAs in gastric cancer. Together with some others, the members of miR-106b-25 cluster showed an upregulated expression pattern when compared with non-tumor samples [115]. Moreover, in this study it was shown that E2F1 controlled expression of miR-106b cluster and in turn, miR-106b and miR-93 regulated the expression of E2F1; so a negative feedback loop exists in this regulation. In addition, by targeting of *CDKN1A (p21)* (a negative cell cycle regulator) miR-93 was found to regulate cell cycle progression in gastric cancer [115]. miR-106b-25 cluster was also correlated with transforming growth factor beta (TGFβ) regulated cell cycle arrest. TGFβ ensures a coordinated cell cycle arrest and induction of apoptosis of mature cells in gastrointestinal tract [116]. Overexpression of miR-93 and miR-106b was shown to interfere with TGFβ dependent G_1-S cell cycle arrest by possibly targeting one or more proteins in this pathway [115]. In another study, *CDKN1A* (*p21)* was shown as direct target of miR-106b in various types of solid tumors (lung, kidney, gastric, colon, breast) [108].

Role of miR-106b-25 cluster was further evaluated by inhibition of *CDKN1A* (*p21)* in esophageal adenocarcinoma. Esophageal cultured cells and tissues were used in this study to have a profile of differentially expressed miRNAs. In association with genomic amplification, miR-106-25 cluster was shown to be up regulated in esophageal adenocarcinoma. Both *in vitro* and *in vivo* studies showed that miR-106b and miR-93 inhibits *CDKN1A* at mRNA level. miR-25, on the other hand, targets *BCL2L11* (*Bim)* (pro-apoptotic gene) and exerts its effect by translational inhibition. By targeting these two important cell-cycle and apoptosis regulators miR-106b-25 was shown to has a potential proliferative, anti-apoptotic, cell cycle promoting and tumorigenic effects [117].

Polisena et al. studied role of miR-106b-25 in prostate tumorigenesis [111]. Tumorigenic effects of these miRNAs were exerted by targeting *PTEN* (Phosphatase and tensin homolog) -a tumor suppressor gene. PTEN inhibits the PI3K-Akt pathway which is a signal transduction pathway taking role in cell survival, cell proliferation, cell motility and angiogenesis. Therefore down-regulation of this protein by miR-106-25 cluster may contribute to the formation of tumors in prostate [111].

The function of miR-106b-25 cluster in cell cycle regulation was explained by *BCL2L11 (Bim)* and *E2F1* targeting in hepatocellular carcinoma (HCC). 56 pairs of HCC samples and the corresponding non-tumor liver samples were analyzed and significant up-regulation of miR-106b-25 cluster was observed. Effect of these miRNAs on cell proliferation was tested via miRNA inhibitors. All three miRNA inhibitors (anti-miR-106b, anti-miR-93 and anti-miR-25) were shown to decrease proliferation in two hepatoma-derived cell lines and one human cervical carcinoma cell line (HeLa). Different from previous studies (gastric cancer, prostate cancer); in HCC *CDKN1A (p21)* did not show a correlation with the expression of miR-106b-25. *BCL2L11 (Bim)* expression on the other hand was higher in tumors that have down-regulated expression of miR-106b-25 cluster. *E2F1* was found to be direct target of miR-106b and

miR-93 in HCC; however E2F1 protein levels were high in miR-106b-25 overexpressing tumors. A possible mechanism was suggested for this finding, such that miR-106b-25 cluster plays a role in regulating E2F1 expression to limit excessive expression, which can result in apoptosis [109].

In another study conducted with laryngeal carcinoma, pro-oncogenic feature of miR-106b was explained by the role of this cluster in cell cycle regulation. Inhibition of miR-106b by antisense oligonucleotides showed a decrease in proliferation of two laryngeal carcinoma cell lines and this inhibition also resulted in G_0/G_1 arrest. Retinoblastoma protein (Rb), which is a tumor suppressor and has a role in G_1/S transition, was shown as direct target of miR-106b [118].

The role of miR-106b-25 cluster in breast cancer was depicted with study of Smith and his colleagues [112]. The relation between miR-106b-25, TGFβ and Homeobox protein SIX1 (Six1) was studied. For the first time, it was shown that miR-106b-25 cluster can target Smad-7 – a TGFβ inhibitor- and activate TGFβ pathway as a downstream effect of *SIX1* overexpression. The overall conclusion from this study enhanced the oncogenic role of this miRNA cluster. miR-106b-25 cluster overcomes TGFβ mediated growth suppression and also promote TGFβ pathway signaling in favor of tumorigenesis. Moreover, for the first time it was revealed that this cluster can induce epithelial-to-mesenchymal transition (EMT) in breast cancer [112]. All of these studies conducted in various types of cancers support the idea of pro-oncogenic ability of miR-106b-25 cluster.

In addition to cancer, miR-106b-25 cluster was also studied in some other pathologies such as Alzheimer's diseases (AD). miR-106b levels were shown to reduce in sporadic AD patients. Lots of evidences suggesting a pivotal role for TGFβ pathway in AD pathogenesis were depicted and direct regulation of expression of TGFβ receptor II (TGFβRII) by miR-106b was shown. Therefore, by involving into TGFβ pathway regulation, miR-106b was possibly playing role in AD pathogenesis [119].

Involvement of miR-106b-25 cluster microRNAs was also reported in induced pluripotent stem cells (iPSC). Together with miR-17-92 and miR-106a-363 cluster, miR-106b-25 cluster was shown to be induced in early reprogramming phases. It was demonstrated that miR-93 and miR-106b improve iPSC programming and regulate mesenchymal-to-epithelial transition step and also inhibition of these miRNAs decline the reprogramming efficiency. It was found that *TGFBR2* and *CDKN1A* (*p21*) are targeted by these miRNAs which improves iPSC induction [120].

1.3 Aim of the Study

Involvement of miRNAs in carcinogenesis of different types of tissues has been reported so far. They have potential to regulate variety of pathways by their tumor suppressing or promoting features. In this study, our aim was to investigate the potential role of miR-106b in breast cancer.

For this purpose, an already constructed non-tumorigenic immortal breast cell line overexpressing miR-106b was used as a model system. Functional assays were performed to examine phenotypical effects of miR-106b in our cell line model.

CHAPTER 2

MATERIALS AND METHODS

2.1 Mammalian Cell Culture Conditions

MCF10A cell line was purchased from ATCC (LGC Standards GmbH, Germany). MCF10A cells were grown in DMEM/Ham's F12 (1:1) medium (Biochrom,AG) containing 5% horse serum (Biochrom,AG), 20 ng/ml Epidermal Growth Factor (EGF) (Sigma), 0.5 µg/ml hydrocortisone (Sigma), 100 ng/ml cholera toxin (Sigma), 10 µg/ml insulin (Sigma) and 1% penicillin/ streptomycin (Biochrom, AG) [121]. MDA-MB-231 cell line was a kind gift from Dr. Uygar Tazebay (Bilkent University, Ankara). MDA-MB-231 cells were grown in Dulbecco's MEM medium containing 10% FBS and 1% penicillin/streptomycin. Serum and penicillin/streptomycin were added into medium after filtrating through 0.22 µm syringe filter (Sartorius Stedium Biotech).

Cells were grown as a monolayer at 37°C with 95% humidified air and 5% CO_2 in a HEPA filtered Heraeus Hera Cell 150 incubator and handled in a Class II laminar flow cabinet by using appropriate cell culture techniques.

Frozen stock vials were thawed in a 37°C water bath. After thawing, the cells were plated into a T-25 flask containing pre-warmed (37°C) appropriate growth medium and incubated at 37°C with 95% humidity and 5% CO_2. After 24 hours, cells were washed with Hank's salt solution (Biochrom,AG) to get rid of dimethyl sulfoxide (DMSO) (Applichem), used for cell storage. According to doubling times of cell lines, media were changed 2-4 times a week and subculturing was done with trypsin-EDTA (Biochrom, AG). Cells were frozen when they reached 90% confluency. 7.5% DMSO was used in corresponding media for long term storage of frozen cells. Cells were frozen and kept at -80 °C for 24 hours and transferred to liquid nitrogen.

All the reagents and chemicals were cell culture grade.

2.2 Transfection of Mammalian Cells

MCF10A cells were used to generate a stable cell line that expressed miR-106b. For this purpose either miR-106b-pSUPER construct or empty pSUPER construct was transfected into cells by using FuGENE HD (Roche) in 3:2 (FuGENE:plasmid) ratio. Generation of miR-106b-pSUPER construct and transfection into MCF10A cells were performed by a previous lab member (Dr. Ayşegül Sapmaz). The map of pSUPER.retro.neo+GFP vector is given in Appendix A.

2.3 Expression Analysis of miR-106b

To detect precursor level of miR-106b (pre-miR-106b) RT-PCR was performed. To measure mature miR-106b expression level, TaqMan microRNA assay (Applied Biosystems) was used.

2.3.1 RNA Isolation by Trizol Reagent

Before RNA isolation, working area was cleaned by RNase away (Molecular Bioproducts) and DNA away (Molecular Bioproducts).

To isolate total RNA, cells were grown in T-75 cell culture flasks until 70-80% confluency. 8 ml TRIzol reagent (Invitrogen) was added onto the cells and samples were incubated at room temperature for 5 minutes to permit complete dissociation of nucleoprotein complexes. The lysates were transferred into a 15 ml sterile tubes and 0.2 ml chloroform per 1 ml of TRIzol (1.6 ml chloroform/T-75 flask) was added. Tubes were shaken vigorously for 15 seconds. After 2-3 minutes of incubation at room temperature, the samples were centrifuged at 4700g for 20 minutes at 8°C. At the end of centrifugation step, RNA remained in the aqueous phase. This phase was transferred into a 15 ml sterile tube and 0.5 ml isopropanol per 1 ml of TRIzol (4 ml isopropanol/T-75 flask) was added into this aqueous solution to precipitate RNA. Samples were incubated at room temperature for 10 minutes and centrifuged at 4700g for 20 minutes at 4°C following the incubation. After this stage, RNA formed a gel-like pellet on the side and bottom of the tube. Supernatant was removed and RNA pellet was washed with 75% ethanol. Sample was mixed by vortexing and centrifuged at 4700g for 10 minutes. Supernatant was discarded and washing step was repeated with 70% ethanol. At the end of last centrifugation step, ethanol was removed carefully and RNA pellet was left at room temperature for 20-30 minutes for drying. Pellet was suspended in 20-50 µl RNase free water and samples were stored at -80°C.

2.3.2 Determination of RNA Quantity and Quality

Concentrations of RNAs were measured by Nanodrop (Thermo Scientific) at 260 nm. 260/280 and 260/230 ratios were checked to assess quality of the samples. For a pure RNA sample, 260/280 ratio should be between 1.8 and 2 and 260/230 ratio should be higher than 1.8 [122].

2.3.3 DNase I Treatment

The RNAs which were used in RT- PCR were treated with Deoxyribonuclease I (DNase I) (Roche) to get rid of DNA contamination in RNA samples. Reaction mixture is listed in Table 2.1.

Table 2.1. DNase I reaction mixture

RNA	5 µg
10 X Reaction Buffer	10 µl
DNase I (10 u/µl)	1.5 µl
RNase-free water	Complete the volume to 100 µl

Reaction mixture was prepared on ice and mixture was incubated in 37°C water bath for 1 hour. Reaction was stopped by adding equal amount of (100 µl) phenol: chloroform: isoamyl alcohol (25:24:1). The solution was vortexed for 30 seconds and incubated on ice for 10 minutes. At the end of incubation period, mixture was centrifuged for 20 minutes at 4°C at 14000g. After centrifugation, upper phase –containing RNA- was taken into a sterile tube. According to volume of upper phase, 1/10 volume of 3 M sodium acetate (NaAc) and 3 volumes of 100% ice-cold ethanol was added and samples were incubated at -20°C overnight for RNA precipitation. At the end of overnight incubation, samples were centrifuged for 30 minutes at 4°C at 14000g. Supernatant was discarded and RNA pellet was washed with 70% ice-cold ethanol and centrifuged for 15 minutes at 14000g. Ethanol was removed carefully and pellet was left to air-dry. RNA pellet was dissolved in 10-30 µl RNase-free water. Success of DNase treatment was tested by PCR, using *GAPDH* primers (Appendix B).

2.3.4 cDNA synthesis

cDNA synthesis was performed by using RevertAid First Strand cDNA synthesis kit (Fermentas). Table 2.2 shows reaction mixture preparation and protocol for the kit.

Table 2.2. Reaction mixture by RevertAid First Strand cDNA synthesis kit and cDNA synthesis protocol.

RNA	1 µg
Primer (random hexamer)	1 µl
Nuclease free water	Add up to 12 µl
Total	12 µl
Briefly centrifuged, incubated at 65°C for 5 minutes, chilled on ice and briefly centrifuged.	
5X Reaction Buffer	4 µl
Ribolock RNase inhibitor (20 u/µl)	1 µl
10 mM dNTP	2 µl
RevertAid Reverse transcriptase (200 u/µl)	1 µl
Total	20 µl
Tubes were mixed and incubated at 25°C for 10 minutes, at 42°C for 60 minutes. Reaction was stopped by heating at 70°C for 5 minutes and chilling on ice.	

2.3.4 Reverse Transcription Polymerase Chain Reaction (RT-PCR)

Precursor miR-106b primers and *GAPDH* primers were used. Sequences of primers are listed in Table 2.3.

Table 2.3. List of primers used in RT-PCR. microRNA primers were precursor structure specific.

Primers		Expected Product Size
GAPDH	Forward: 5′-GGGAGCCAAAAGGGTCATCA-3′	407 bp
	Reverse: 5′-TTTCTAGACGGCAGGTCAGGT-3′	
hsa-miR-106b	Forward: 5′-CCTGCCGGGGCTAAAGTGCT-3′	80 bp
	Reverse: 5′-TGCTGGAGCAGCAAGTACCCA-3′	

Reaction mixture for pre-miR-106b reaction or *GAPDH* reaction is given in Table 2.4.

Table 2.4. RT-PCR mixture to amplify pre-miR-106b and *GAPDH*.

Molecular grade water	14.35 µl
10 x reaction buffer	3 µl
dNTP mix(2 mM each)	3 µl
Forward primer (GAPDH or hsa-miR-106b) (5 µM)	3 µl
Reverse primer (GAPDH or hsa-miR-106b) (5 µM)	3 µl
$MgCl_2$ (25mM)	2.4 µl
Taq polymerase (1 u/µl) (Fermentas)	0.25 µl
cDNA	1 µl
TOTAL	30 µl

Cycling conditions for *GAPDH* PCR and hsa-miR-106b PCR are given in Table 2.5.

Table 2.5. RT-PCR cycling conditions for *GAPDH* and hsa-miR-106b.

95°C	2:00 min	
95°C	0:30 min	30 cycles
62°C	0:30 min	
72°C	0:30 min	
72°C	10:00 min	
4°C	infinite	

15 µl PCR product was loaded onto 2% agarose gel and electrophoresed at 100V. Ethidium bromide was used for visualization of DNA under UV.

2.3.4.1 Densitometry Analysis of RT-PCR

RT-PCR agarose gel images were analyzed using Image J program (NIH). Fold changes calculated from empty vector transfected cDNAs for *GAPDH* and hsa-miR-106b intensities were used to normalize fold changes of miR-106b transfected cDNAs. Formula that was used for this calculation is given below.

$$\text{Fold Change} = \frac{\text{hsa} - \text{miR} - 106\text{b transfected (miRNA}/GAPDH)}{\text{empty vector transfected (miRNA}/GAPDH)}$$

2.3.5 Detection of mature miR-106b levels

To detect mature miR-106b level in MCF10A-EV (empty pSUPER transfected MCF10A cells) and MCF10A-106b cells (pSUPER containing pre-miR-106b sequence transfected MCF10A cells), TaqMan® microRNA assay (Applied Biosystems) was performed. RNAs from MCF10A-EV and MCF10A-106b cells were isolated by using TRIzol reagent (as stated in part 2.3.1). RNAs without DNase treatment were used to synthesize cDNA by TaqMan® microRNA Reverse Transcription Kit. cDNA synthesis reaction mixture and protocol are summarized in Table 2.6. cDNA synthesis was performed both for miR-106b and small nuclear RNA U6 , *RNU6B* (reference gene). There are separate RT primers for miR-106b and RNU6B. This assay was performed twice with a total of 6 replicates.

Table 2.6. TaqMan cDNA synthesis reaction mixture and protocol.

Component	**Volume**
100 mM dNTPs	0.15 µl
Reverse transcriptase (50 u/µl)	1.00 µl
10x Reverse transcription buffer	1.50 µl
RNase inhibitor (20 u/µl)	0.19 µl
Water	4.16 µl
Total	7.00 µl
Mix and centrifuge the mixture and place it on ice.	
Take 7 µl RT mix into tubes and add 5 µl RNA (100 ng). Mix and centrifuge. Add 3 µl 5X RT primer (either miR-106b or RNU6B).	
Put the mixture on ice and wait for 5 min.	
Start the reaction; 30 min at 16 °C , 30 min at 42 °C , 5 min at 85 °C, 4 °C store. Use freshly synthesized cDNAs in the reaction.	

After synthesizing the cDNAs, TaqMan qRT-PCR mix was prepared. Two different reaction mixtures were prepared; for miR-106b and for RNU6B. For miR-106b qRT-PCR, cDNAs synthesized by using miR-106b RT primer were used. For *RNU6B* qRT-PCR cDNAs synthesized by using *RNU6B* RT primer were used. Reaction mixture was prepared as stated in Table 2.7.

Table 2.7. TaqMan qRT-PCR mixture.

Component	**Volume**
TaqMan Small RNA assay 20x	0.5 µl
TaqMan Universal PCR Master Mix (2x)	5 µl
cDNA (from RT reaction)	0.665 µl
water	3.835 µl
TOTAL	10 µl

TaqMan Small RNA assay (20x) differs for miR-106b and RNU6B. Therefore two different reaction mixes were prepared. Four dilutions of cDNA were used as standards; no dilution, 1:2, 1:4 and 1:10. Cycling conditions were same for RNU6B and miR-106b (Table 2.8). qRT-PCR was performed by using Rotor Gene 6000 (Corbett, Qiagen) cycler. MIQE guidelines were followed in qRT-PCR experiment [123] (Appendix C).

Table 2.8. Thermal cycling conditions for TaqMan qRT-PCR.

94 °C	10:00 min	
94 °C	0:15 min	} 40 cycles
60 °C	1:00 min	

cDNA synthesis and qRT-PCR are summarized in Figure 2.1.

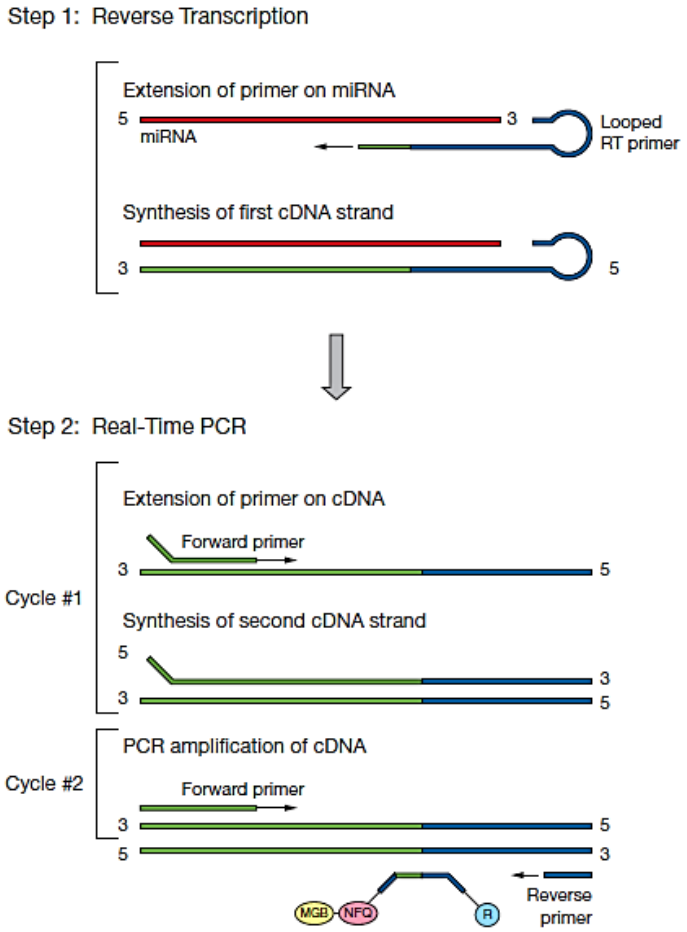

Figure 2.1. First strand cDNA synthesis with looped RT primer and real time PCR with gene specific forward primers and loop specific reverse primer (Taken from http://tools.invitrogen.com/content/sfs/manuals/cms_042167.pdf).

Assay chemistry is summarized in Figure 2.2.

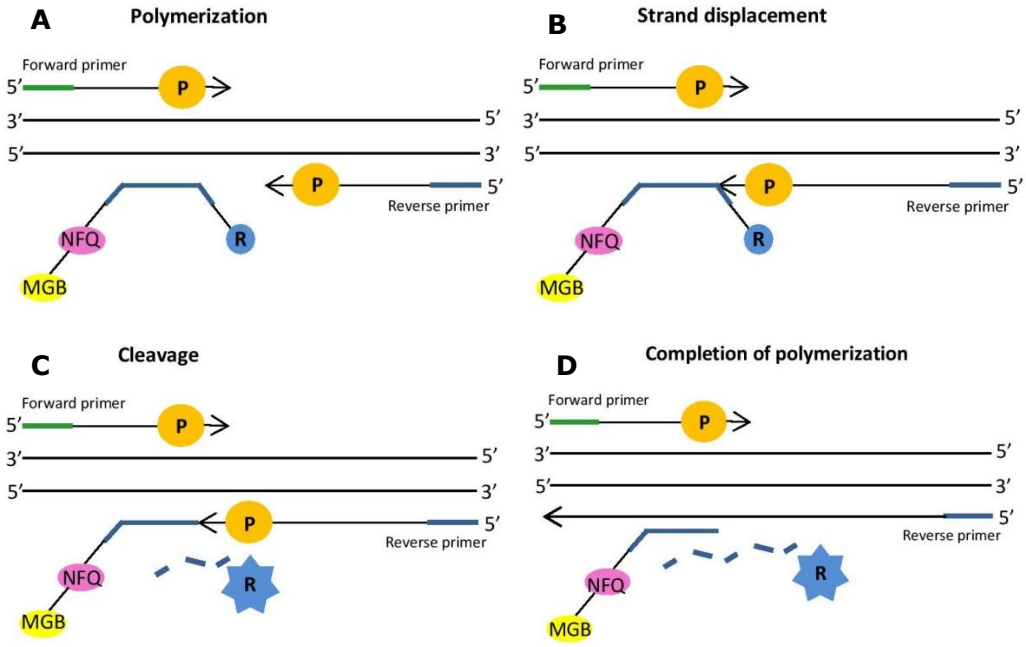

Figure 2.2. 5′ nuclease assay process. NFQ: Nonfluorescent quencher, MGB: Minor groove binder, R: Reporter, P: Hot-start DNA polymerase. **A-B.** MGB probe anneals specifically to a complementary sequence between forward and reverse primers. When probe is intact, quencher dye suppress the fluorescence of reporter dye. **C.** Probes that are hybridized to target are cleaved by DNA polymerase. As a result reporter dye is separated from quencher dye and this separation cause an increase in fluorescence by the reporter. **D.** Strand polymerization occurs, since 3′ end of the probe is blocked, probe extension is not possible during PCR (Taken from http://tools.invitrogen.com/content/sfs/manuals/cms_042167.pdf).

2.3.5.1 Analysis of TaqMan qRT-PCR results

The reaction efficiency incorporated ΔΔCt formula was used for relative quantification analysis [124]. Equation is stated below (E stands for the efficiency of reaction, R stands for relative expression ratio). Three independent biological replicates with three technical replicates per experiment were used for each qRT-PCR. The fold change was normalized against reference gene *RNU6B*. Statistical analysis was performed by using GraphPad Prism program, for analysis t-test was used.

$$R = \frac{(E\ target\ )^{\Delta Ct\ target\ (control-sample)}}{(E\ reference)^{\Delta Ct\ reference\ (control-sample)}}$$

2.4 Functional Assays

2.4.1 Growth curve analysis

10^4 cells per well from both MCF10A-EV and MCF10A-106b were seeded on to 24 well plates. This starting point was defined as Day 0. Cells were trypsinized and counted at days 0, 1, 3, 5 and 7 by the aid of a hemocytometer. Based on counted cell numbers graph was plotted by using GraphPad Prism.

2.4.2 Cellular Proliferation Assay

To determine the effect of miR-106b on proliferation of cells, MTT cell proliferation assay was performed. The assay is based on conversion of yellow tetrazolium salt MTT (3-(4,5-dimethylthiazol-2-yl)-2,5-diphenyltetrazoliumbromide) into insoluble purple formazan crystals by mitochondrial reductase of viable cells [125] (Figure 2.3). For the solubilization of formazan crystals, 10% SDS in 0.01 M HCl solution was used and concentration of solubilized product was determined by optical density at 570 nm. This experiment was performed three times with a total of 27 technical replicates.

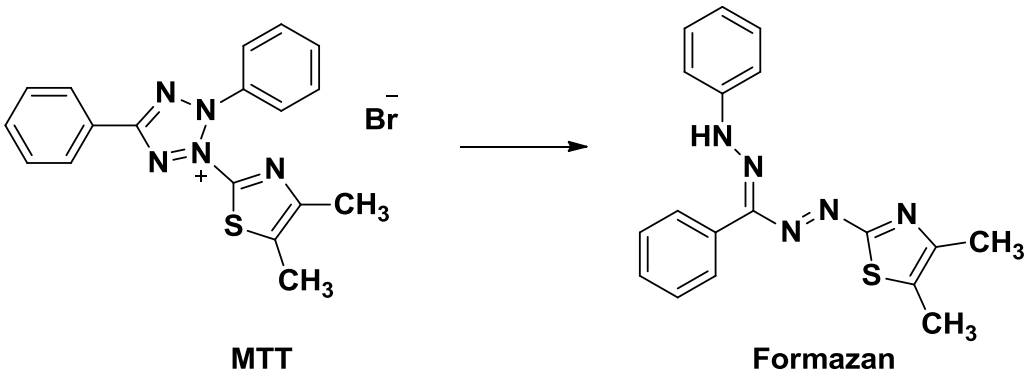

Figure 2.3. Cleavage of MTT to formazan salt (Cell Proliferation Kit I (MTT), Roche).

$5x10^3$ MCF10A cells were seeded into 96 well plates in complete growth medium. For 0 hour time point, after cells attached to the surface of plates 10 µl MTT solution was added and after 4 hours of incubation 100 µl solubilization buffer was added to solubilize formazan crystals. Absorbance was measured at 570 nm by Bio-Rad microplate reader at the end of overnight incubation at 37 °C. For 24,48,72 and 96 hour time points, MTT solution was added 24,48,72 and 96 hours after seeding, respectively. The

rest of the procedure was same with that of 0 hour plate. The medium with MTT was used as blank for microplate reading.

2.4.3 *In vitro* Wound Closure Assay

To examine directional migration ability of the cells, *in vitro* wound closure assay was performed [126]. MCF10A-EV and MCF10A-106b cells were seeded into 6 well plates and grown until they reached 90% confluency. A wound was introduced to the cells by scratching the monolayer by the aid of 1000 µl pipet tip. To get rid of cell debris, washing was performed with Hank's Salt solution twice. Cells were then grown in complete growth medium. Wound areas were marked with a permanent marker to determine the initial size of the wound. An image was taken right after introducing the wound and cells were left to grow. Images were taken at 12, 24, 36 and 48 hours after the wounding process. Cells were observed under Olympus phase contrast microscope by using 4X objective (total magnification 40X) and Moticam 2300 camera system attached to the microscope was used to capture images. Distances travelled by the cells were measured by Motic ImagePlus 2.0 software. This assay was performed three times with a total of six replicates.

2.4.4 Transwell migration assay

Transwell migration assay was performed to assess the migration ability of the MCF10A-EV and MCF10A-106b cells. Migration assay was performed in 24-well plates using migration chambers from Greiner Bio-one. Representation of chamber is shown in Figure 2.4.

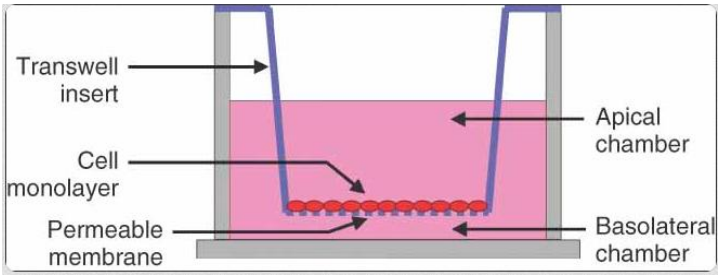

Figure 2.4. Illustration of transwell chamber. Cells were seeded into apical chamber and let to migrate through permeable membrane (Taken from [127]).

The rationale behind this assay was to starve the cells so that they would tend to migrate through the pores of the membrane to reach the medium that contains more growth factors. Cells were pre-starved in low serum containing medium (medium containing 1% horse serum) for 24 hours. After starvation

$7x10^4$ cells were seeded onto upper chamber of transwell in 100 µl 1% serum containing medium. 600 µl complete medium (5% horse serum) containing 5 µg/ml fibronectin was added to lower chamber (marked as basolateral chamber in Figure 2.4). Cells were let to migrate for 24 hours through a 8 µm pore membrane. At the end of this period, cells on the upper surface of the membrane were removed by the aid of a cotton swab. For the fixation of the cells on the lower surface 100% methanol was used and chamber were incubated in methanol for 10 minutes. Fixed cells were stained with Giemsa for 2 minutes and membranes were washed three times with distilled water. After complete drying of membranes, they were cut out and mounted onto a glass slide upside down position with a drop of paraffin oil. Cells on the upper side of membrane were counted under a Leica light microscope at 40x objective (total magnification 400x). This assay was performed three times with a total of six replicates.

2.4.5 Matrigel Invasion assay

Matrigel (BD Biosciences) is a basement membrane matrix extracted from Engelbreth-Holm-Swarm (EHS) mouse sarcoma and contains laminin, collagen IV, heparin sulfate proteoglycans, TGF-β, epidermal growth factor, insulin-like growth factor, fibroblast growth factor, tissue plasminogen activator and some other growth factors which are naturally found in EHS tumor [128]. Matrigel is used in several types of tumor cell invasion assays [129].

To investigate invasion properties of MCF10A-EV and MCF10A-106b cells, matrigel invasion assay was performed. MDA-MB-231 cells were used as positive control for invasion. Assay principle is the same with migration assay. Different from migration assay invasion assay has matrigel mimicking the basement membrane. Matrigel was diluted 1:5 with serum free growth medium and 100 µl diluted matrigel was added into upper chamber of each transwell. For solidification of matrigel, inserts were incubated at 37 °C for 4-5 hours. Pre-starved cells were seeded onto the matrigel containing transwell insert. $7x10^4$ cells in 100 µl 1% serum containing medium were seeded. Cells were let to invade for 24 hours and at the end of this step, fixation and staining procedures were applied to the membrane as described in section 2.4.3. Cells on the upper side of membrane were counted under a Leica light microscope at 40X objective (total magnification 400X). This assay was performed three times with a total of six replicates.

CHAPTER 3

RESULTS AND DISCUSSION

3.1 Generation of miR-106b overexpressing stable breast cell line

To study the effects of miR-106b overexpression in breast cancer cell lines, a miR-106b overexpression model cell line was generated and used. MCF10A cell line is a non-tumorigenic breast epithelial cell line that is obtained from a 36 year old Caucasian female [130]. Expression level of pre-miR-106b in MCF10A cells was shown by qRT-PCR to be similar to normal breast tissue by Dr. Ayşegül Sapmaz in our laboratory. Hence MCF10A cell line was chosen to be transfected with a pre-miR106b overexpressing construct. Construction of stable cell line was performed as described in materials and methods section by Dr. Ayşegül Sapmaz (section 2.2).

3.2 Expression analysis of pre-miR106b in MCF10A-EV and MCF10A-106b cells

Polyclones from empty vector (MCF10A-EV) and pre-miR-106b (MCF10A-106b) overexpression vector transfected cells were selected. To check the success of transfection, miR-106b levels were analyzed. As a first step pre-miR-106b (precursor miRNA transcript) expression was checked by RT-PCR. *GAPDH* primers were used as housekeeping control gene (407 bp) in a separate PCR. After agarose gel electrophoresis of the PCR products, densitometry analysis was performed via Image J program (National Institute of Health). Band intensities of miRNA/*GAPDH* PCR products were determined for MCF10A-EV and MCF10A-106b and value of MCF10A-106b was normalized to that of MCF10A-EV (Figure 3.1).

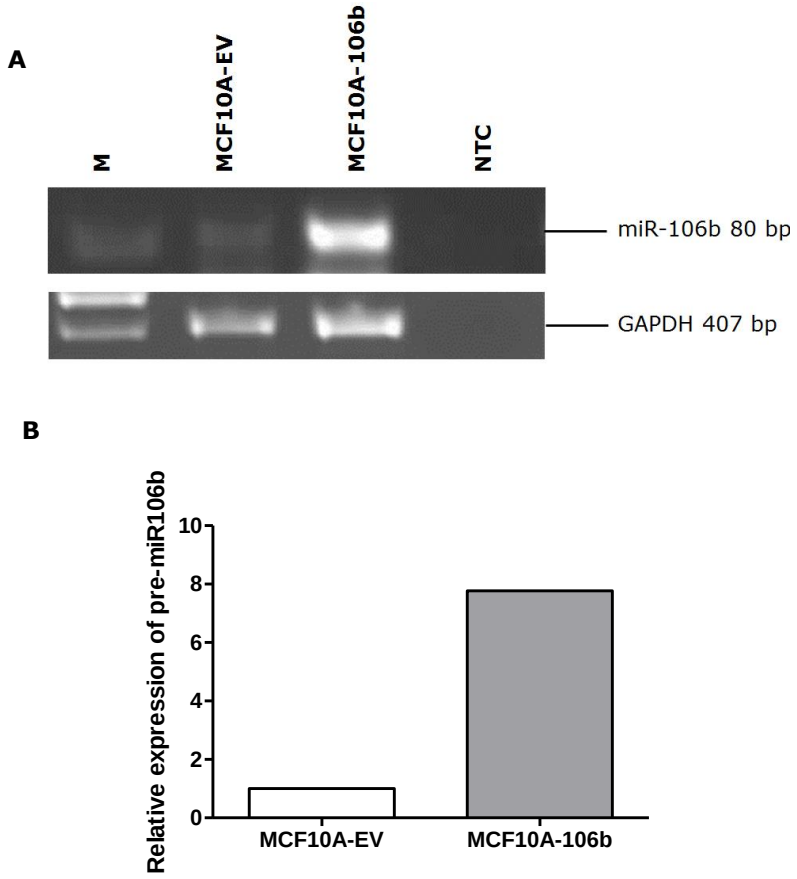

Figure 3.1. pre-miR-106b expression analysis by RT-PCR in MCF10A-EV and MCF10A-106b cells. **A.** Agarose gel image of 80 bp pre-miR-106b and 407 bp *GAPDH* PCR products. **B.** Densitometry results were normalized according to miRNA/*GAPDH* band intensity value of MCF10A-EV and it was set to 1 (M:Marker, NTC: No template control).

According to RT-PCR, MCF10A cells that were transfected with pre-miR-106b vector, expressed 7.7 fold more pre-miR-106b compared to MCF10A-EV cells. Since pre-miRNA levels may not always correlate with mature levels, we analyzed mature miRNA levels in MCF10A-EV and MCF10A-106b cells to confirm the overexpression.

3.3 Expression of mature miR-106b in MCF10A-EV and MCF10A-106b cells

Mature miR-106b levels were detected by TaqMan microRNA assay according to manufacturer's instructions (Applied Biosystems) as described in section 2.3.5. For relative quantification, expression level of miR-106b in MCF10A-EV

cells was set to 1. The fold change was normalized against the reference gene, small nuclear RNA U6 (*RNU6B*) (Figure 3.2).

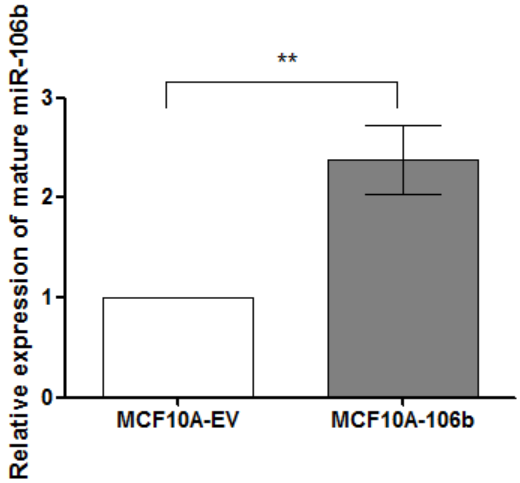

Figure 3.2. Mature miR-106b levels in MCF10A-EV and MCF10A-106b cells. Expression level was detected using TaqMan miRNA assay. Reaction efficiency incorporated ΔΔCt formula [124] was used for quantification. The baseline was set to 1 in MCF10A-EV cells. Error bar represents the SD of two independent experiments with a total of six technical replicates. ** indicates significant difference, $p<0.01$ (t test).(One replicate of this assay was performed by Shiva Akhavantabasi).

The result of TaqMan microRNA assay clearly showed 2.4 fold increase in mature miR-106b level in MCF10A-106b cells compared MCF10A-EV cells. This polyclone was used in further assays.

3.4 Functional assays

To understand the effect of miR-106b expression in MCF10A cells, assays related with proliferation, migration and invasion were performed.

3.4.1 Cellular Proliferation

3.4.1.1 Growth curve analysis

To examine the effect of miR-106b in cell proliferation, 10^4 MCF10A-EV and 10^4 MCF10A-106b cells were plated on a 24 well plate. Cells were counted on days 1, 3, 5 and 7. Day 0 indicates the cell number at starting point (Figure 3.3).

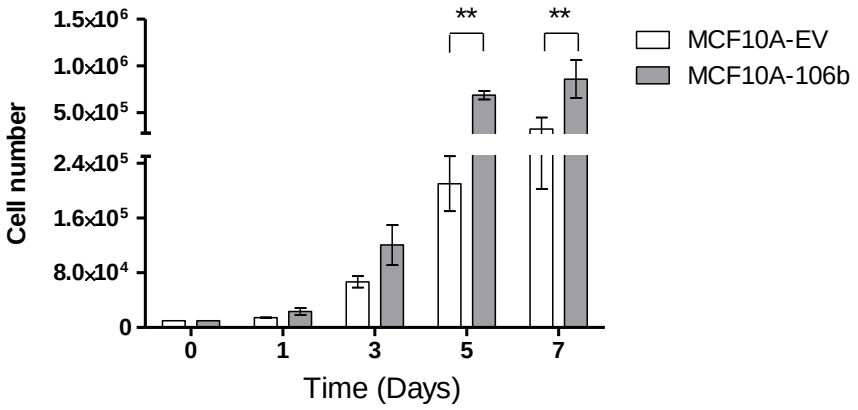

Figure 3.3. Growth curve for MCF10A-EV and MCF10A-106b cells. 10^4 cells were seeded and recorded as Day 0. Error bars represent SD of three independent experiments with a total of six replicates. ** indicates significant difference between MCF10A-EV and MCF10A-106b, $p<0.01$ (two-way ANOVA followed by Bonferroni posttest).

As a result of growth curve analysis, it was concluded that MCF10A-106b cells proliferate approximately 2.6 fold more than MCF10A-EV cells (Figure 3.3).

3.4.1.2 Cellular Proliferation Assay (MTT)

Role of miR-106b on cell proliferation was further investigated by MTT assay for MCF10A-EV and MCF10A-106b cells. Assay was performed according to manufacturer's instructions (Roche). MTT assay is used to determine metabolically active cells [125]. Therefore, by comparing metabolic activity, proliferation rate of cells was inferred. The result of this assay is shown in Figure 3.4.

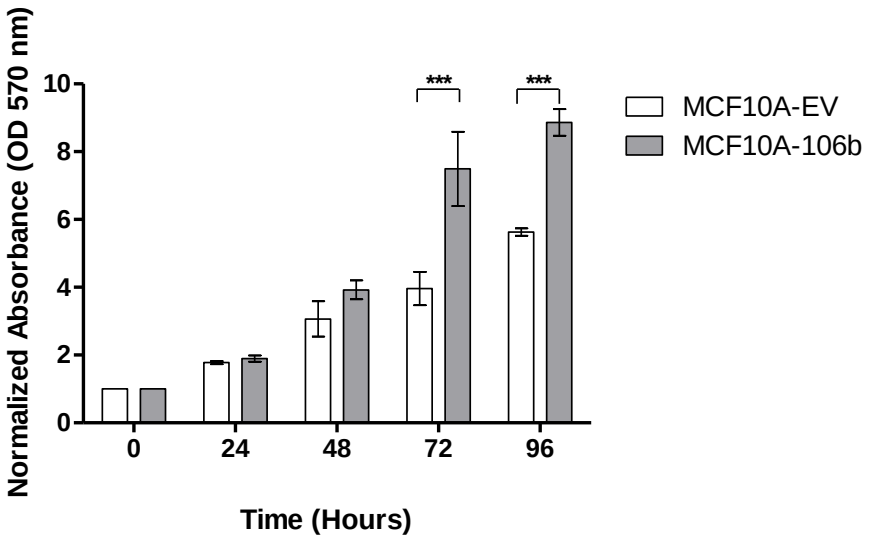

Figure 3.4. MTT assay for MCF10A-EV and MCF10A-106b cells. Error bars represent SD of three independent experiments with a total of 27 replicates. $5x10^3$ MCF10A-EV and $5x10^3$ MCF10A-106b cells were seeded in 96 well plates in MCF10A growth medium. Absorbances were normalized to that of Day 0. *** indicates significant difference in proliferation between MCF10A-EV and MCF10A-106b $p<0.001$ (two-way ANOVA followed by Bonferroni posttest).

Starting from 72nd hour, a significant difference in rate of proliferation between MCF10A-EV and MCF10A-106b cells was observed. At the end of 96th hour, proliferation rate of MCF10A-106b was 1.57 fold more compared to MCF10A-EV cells. Similar results indicating increase in proliferation rate upon miR-106b transfection has been shown in several studies. In laryngeal carcinoma cell lines, transfection of miR-106b resulted in increased proliferation rate [118]. Similar results were obtained in mammary epithelial cells [108], esophageal adenocarcinoma [117], hepatocellular carcinoma [109], prostate cancer [111] and breast cancer cells [112]. Consistent with these results; when inhibited, decreased levels of miR-106b resulted with decreased proliferation rate [108,109,117]. Therefore, based on our MTT result and earlier literature on higher proliferation rate upon miR-106b transfection, our model system was further used for other functional assays.

3.4.2 Directional Migration Phenotype

In vitro wound closure assay is used to investigate directional cell migration [126]. This assay mimics the cell migration during wound healing process *in vivo* [131]. After cells reach 90% confluency, a wound was introduced with a sterile pipet tip and distances travelled by the cells in wound closure process were tracked until wound was closed by MCF10A-106b cells (Figure 3.5).

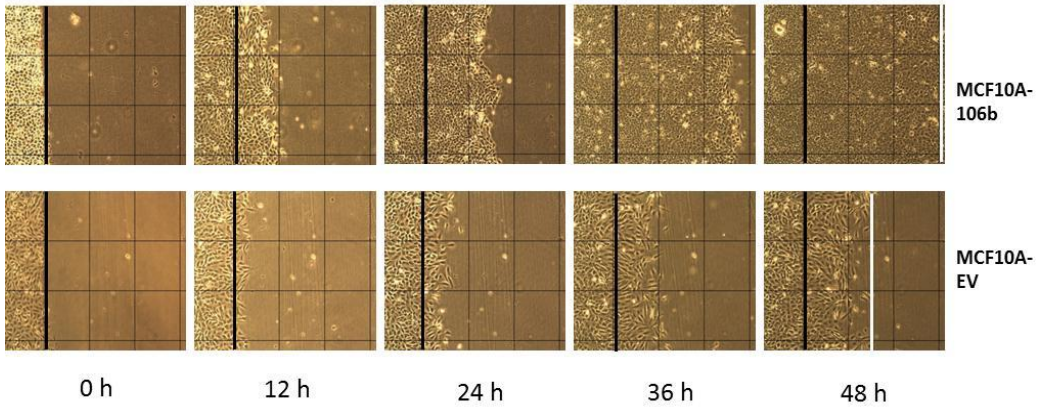

Figure 3.5. Representative wound healing images of MCF10A-106b and MCF10A-EV (total magnification: 40X). Black bars indicate initial wound location. White bars indicate the final location that cells travelled at the end of 48 hours.

After 48 hours of introducing the wound, MCF10A-EV cells were not able to close the wound. On the other hand, MCF10A-106b cells closed the gap at the end of 48 hours which indicated an increase in directional migration capacity of MCF10A cells upon miR-106b expression.

The images were taken every 12 hours by an inverted microscope with a 4X objective. Distances travelled by the cells were calculated in terms of percentage and graph was obtained by using GraphPad Prism Software as shown in Figure 3.6.

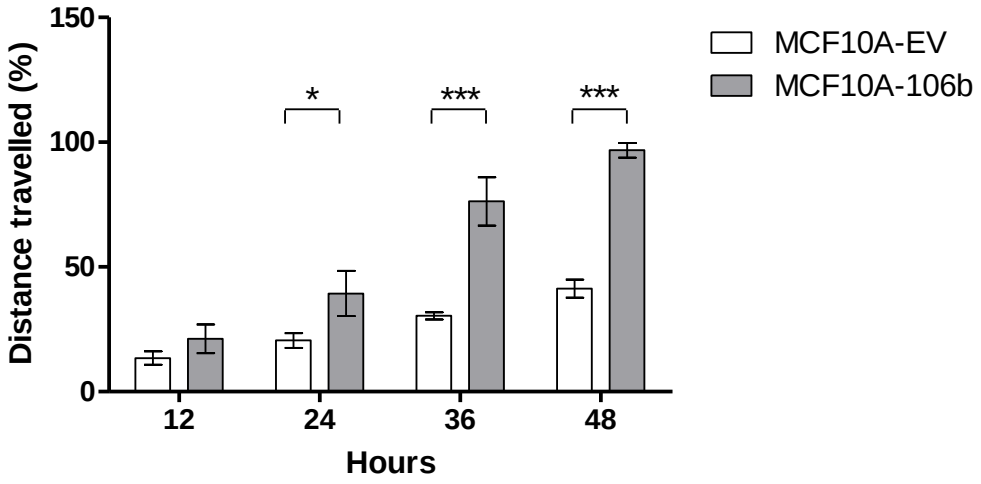

Figure 3.6. Distance travelled by MCF10A-106b and MCF10A-EV cells. Error bars represent the SD of three independent experiments with a total of six replicates. * indicates significant difference when $p<0.05$, ** indicates significant difference when $p<0.01$, *** indicates significant difference when $p<0.0001$ between MCF10A-EV and MCF10A-106b (two-way ANOVA followed by Bonferroni posttest).

The result of this assay showed that, miR-106b caused an increase in motility of MCF10A cells. Directional migration ability reflects migration ability of cells *in vivo*. Therefore by wound healing assay, migration ability of cells *in vivo* might be predicted.

Supporting our results; an enhanced cell migration was shown in miR-106b transfected MCF7 cells by wound healing assay in a recent study [132]. In addition to this, another member of miR-106b-25 cluster, miR-93 (same seed sequence with miR-106b), was shown to increase the migration ability of endothelial cells by targeting integrin-β8 [133]. Since miR-106b and miR-93 have same seed sequence, enhanced cell migration phenotype upon miR-106b expression could be explained by shared targets with miR-93.

3.4.3 Transwell migration assay

Invasion and metastasis are among the hallmarks of cancer as defined by Hanahan and Weinberg [70]. With the rearrangement of cytoskeletal composition cells gain ability to migrate [134]. To compare the migration abilities of MCF10A-EV and MCF10A-106b cells, transwell migration assay was performed. Cells were pre-starved in 1% serum containing growth media for 24 hours and then seeded onto upper chamber of transwell insert. The lower chamber contained complete growth medium (5% serum). After 24 hours, membranes were fixed and stained. Migrated cells were counted under a Leica light microscope (40x objective) (Figure 3.7).

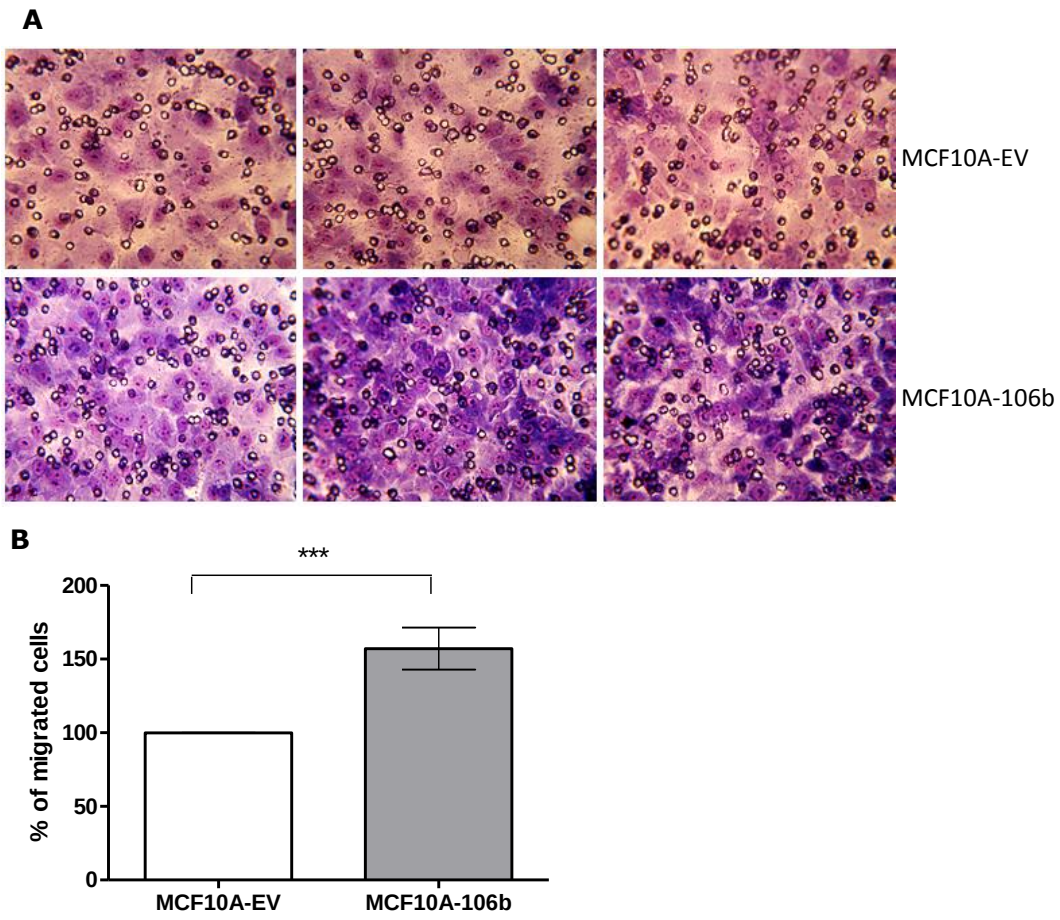

Figure 3.7. Migration assay for MCF10A-EV and MCF10A-106b cells. **A.** Representative images of MCF10A-EV and MCF10A-106b cells migrated through membrane. Total magnification of images 400X. **B.** Percentage of migrated cells through membrane at 24 hour. MCF10A-EV was set to 100%. Error bar represents the SD of three independent experiments with a total of six technical replicates. *** indicates significant difference between MCF10A-EV and MCF10A-106b $p<0.001$ (t test).

This data showed that presence of miR-106b in MCF10A cells caused a 1.6 fold increase in migration of these cells. This transwell migration assay was performed in complete growth medium of MCF10A cells (serum percentage was decreased to 1%). As it was stated in materials and methods section, growth medium of MCF10A cells contain many additives including Epidermal Growth Factor (EGF). MCF10A cells are known to express EGF Receptor (EGFR) [135]. EGF is required for the growth of MCF10A cells [121] and EGF is a well-known migration stimulating agent [136,137,138]. To investigate the impact of EGF on cell motility in MCF10A cells, migration assay in the absence of EGF was performed. Cells were starved in medium lacking EGF. Pre-starved cells were seeded onto the upper chamber of transwell inserts. After 24 hours,

membranes were fixed and stained. Migrated cells were counted under a Leica light microscope (40X objective) (Figure 3.8).

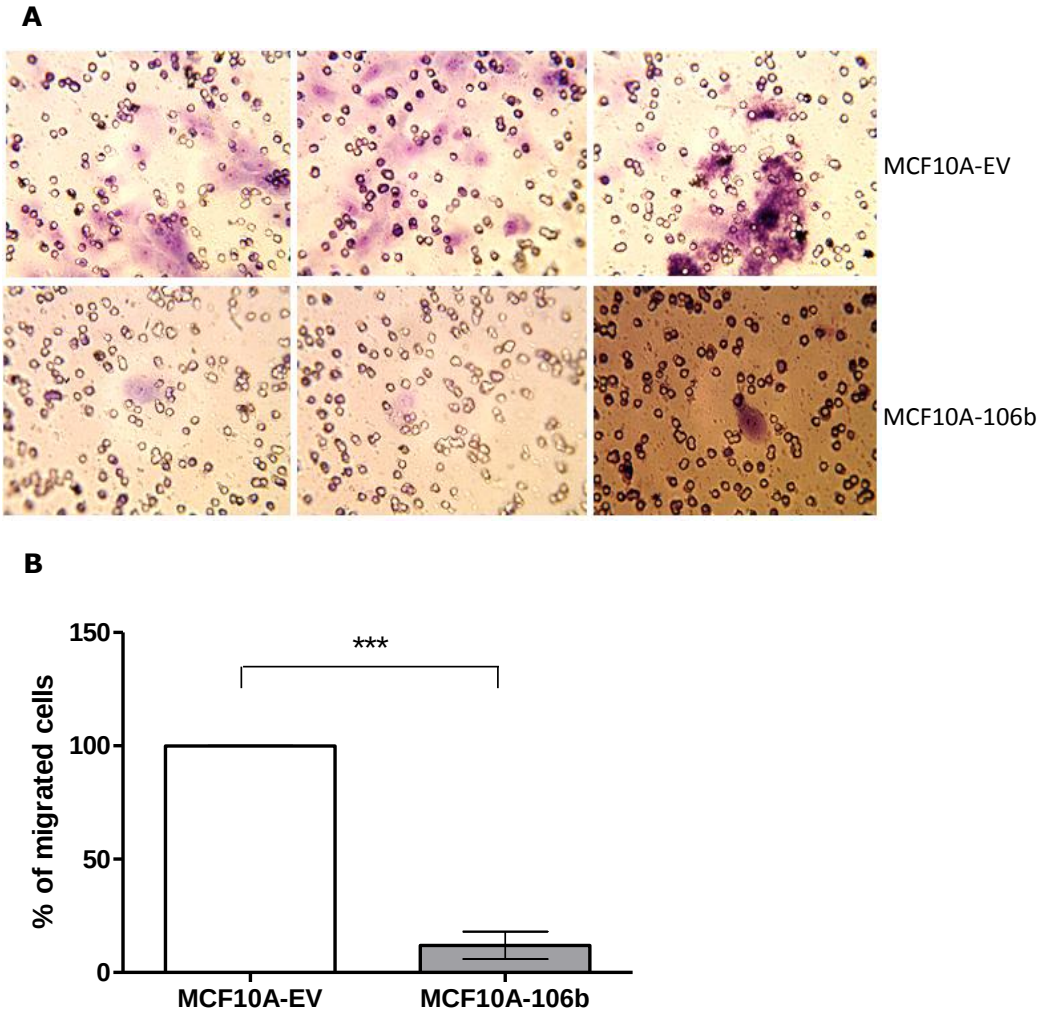

Figure 3.8. Migration assay for MCF10A-EV and MCF10A-106b cells in the absence of EGF. **A.** Representative images of MCF10A-EV and MCF10A-106b cells migrated through membrane. Total magnification of images 400X. **B.** Percentage of migrated cells through membrane at 24 hour. MCF10A-EV was set to 100%. Error bar represents the SD of three independent experiments with a total of six technical replicates. *** indicates significant difference between MCF10A-EV and MCF10A-106b $p<0.0001$ (t test).

Migration assay that was performed in the absence of EGF, showed an opposite pattern to those performed in the presence EGF. In the absence of EGF, MCF10A-106b cells migrated 90% less compared to MCF10A-EV cells. This decrease in migration of MCF10A-106b cells in the absence of EGF might

suggest an interaction between miR-106b and EGF pathways. Moreover, a general decrease in the migration of cells in the absence of EGF should be noted.
In a previous study, MCF10A cells were used as a model to explain EGF driven cell migration in mammary cells [139]. In parallel to our results, Katz et al. showed that EGF induces the migration of MCF10A cells; whereas absence of EGF suppresses migration [139]. EGF induced cell migration was explained by actin cytoskeleton reorganization [139,140] and by ERK/MAPK pathway[141] in MCF10A cells. Since the arrangement of cytoskeletal elements is important in migration, Katz et al. tried to clarified molecules involved in this rearrangement. TNS3 (tensin-3) and TNS4 (CTEN) are two focal adhesion related proteins [142] and their expression levels were found to be changed upon EGF treatment. TNS3 was downregulated whereas TNS4 expression was upregulated when cells were grown in EGF containing medium. Upregulation of TNS4 and downregulation of TNS3 together promote migration by the disassembly of actin fibers [139]. In our data, increased migration of MCF10A-106b cells in the presence of EGF might be explained by both EGF induction and specific targeting by miR-106b. For instance, it is predicted that TNS-3 (in FindTar3) is targeted by miR-106b. Therefore downregulation of TNS-3 by both EGF and miR-106b might contribute migration of cells. On the other hand, decreased migration of MCF10A-106b compared to MCF10A-EV, in the absence of EGF, might possibly resulted from different regulation of miR-106b target mRNAs when EGFR signaling pathway is not active.

To investigate correlation between proliferation and migration in the absence of EGF, MTT assay was performed in medium lacking EGF. Since MCF10A-106b cells migrate less in the absence of EGF, we wondered whether there is any difference in proliferation of these cells, as well. MTT was performed as described in section 2.4.2, without EGF in the growth medium. Result of this assay is shown in Figure 3.9.

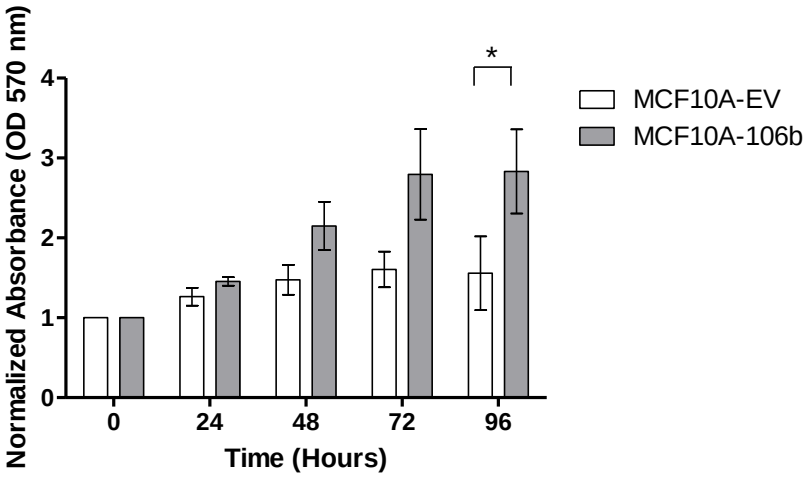

Figure 3.9. MTT assay of MCF10A-EV and MCF10A-106b cells in the absence of EGF. Error bars represent SD of three independent experiments with a total of 27 replicates. $5x10^3$ MCF10A-EV and $5x10^3$ MCF10A-106b cells were seeded in 96 well plates in MCF10A growth medium lacking EGF. * indicates significant difference in proliferation between MCF10A-EV and MCF10A-106b $p<0.05$ (two-way ANOVA followed by Bonferroni posttest).

MTT data showed that, also in the absence of EGF, MCF10A-106b cells proliferated more than MCF10A-EV cells. It should also be noted that in the absence of EGF, general proliferation rate of both MCF10A-EV and MCF10A-106b cells decreased compared to cells grown in the presence of EGF.

In addition to the different pattern in migration, morphology of MCF10A-106b cells changed in the absence of EGF (Figure 3.10).

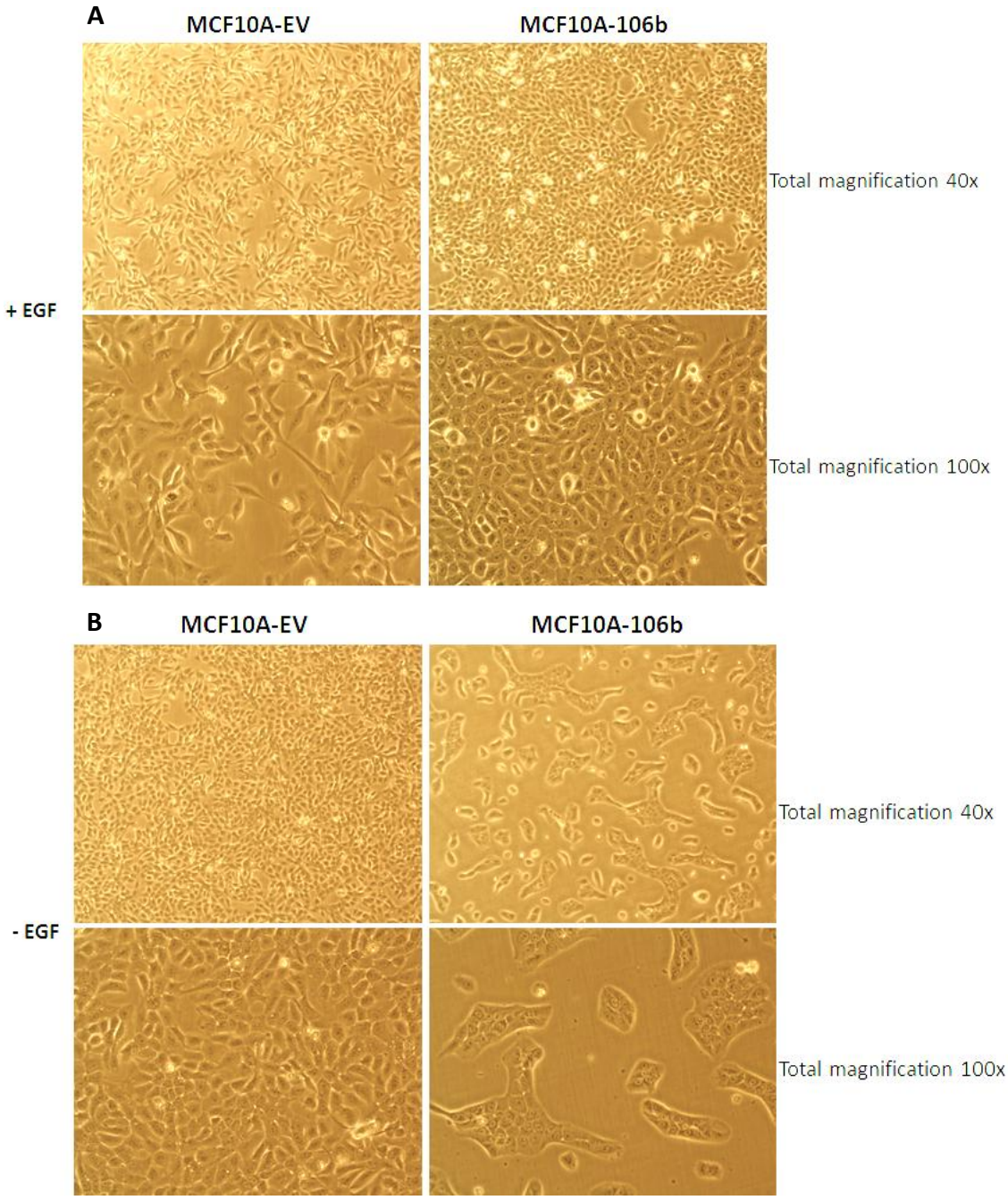

Figure 3.10. Images of MCF10A-EV and MCF10A-106b cells after 24 hours starvation in medium containing 1% serum. **A.** Cells were grown in medium containing EGF. **B.** Cells were grown in medium lacking EGF. Upper panel in each figure shows the cells under 4X objective (total magnification 40X), closer images were taken under 10X objective (total magnification 100X).

MCF10A-106b cells started to grow as clusters, in the absence of EGF, when compared to MCF10A-EV cells. When MCF10A-106b cells were grown in medium lacking EGF, they formed dense cell clusters. In accordance with this observation, clustered morphology of MCF10A cells in the absence of EGF was shown in a study conducted in MCF10A cells[139]. Showing the cluster appearance in MCF10A-106b but not in MCF10A-EV cells might be explained by miR-106b targets related with arrangement cytoskeletal elements.

Different behavior of MCF10A-106b cells in the absence and presence of EGF, might indicate a cross-talk between EGF and miR-106b pathways. EGF receptors promote cell survival, growth and differentiation via the activation of several integrated signaling pathways [143]. According to miRNA-mRNA target prediction programs (TargetScan, PITA, FindTar3) some of the members in EGF pathway [144] were predicted to be targeted by miR-106b such as *STAT3* and *AKT3* (Figure 3.11 and Figure 3.12).

A

Conserved

	predicted consequential pairing of target region (top) and miRNA (bottom)	seed match	site-type contribution	3' pairing contribution	local AU contribution	position contribution	context+ score
Position 158-164 of STAT3 3' UTR hsa-miR-106b	5' ...CUUUGAGCAAUCUGGGCACUUUU... 3' UAGACGUGACAGUCGUGAAAU	7mer-m8	-0.120	-0.007	-0.023	-0.039	-0.14
Position 448-454 of STAT3 3' UTR hsa-miR-106b	5' ...CAUACUCCUGGCAUUGCACUUUU... 3' UAGACGUGACAGUCGUGAAAU	7mer-m8	-0.120	-0.007	-0.060	0.002	-0.14

Poorly Conserved

	predicted consequential pairing of target region (top) and miRNA (bottom)	seed match	site-type contribution	3' pairing contribution	local AU contribution	position contribution	context+ score
Position 623-629 of STAT3 3' UTR hsa-miR-106b	5' ...ACGCCUGUAAUCCCAGCACUUUG... 3' UAGACGUGACAGUCGUGAAAU	7mer-m8	-0.120	0.012	0.074	0.026	> -0.02

B

Organism	Gene Name	microRNA	Position	Seed	dGduplex	dGopen	ddG	Conservation
Human	STAT3	hsa-miR-106b	259	7:0:0	-16.06	-9.29	-6.76	0.99
Human	STAT3	hsa-miR-106b	724	8:0:0	-19.3	-12.93	-6.36	0
Human	STAT3	hsa-miR-106b	549	7:0:0	-12.5	-8.07	-4.42	0.82

C

miRNA	mRNA	Position	Structure	Loop Score	ΔG	Recommendation
hsa-miR-106b	NM_003150	141-165	3' UAGACGUGACAGUCGUGAAAU 5' 5' TTGAGCAATCTGGGCACTTTT 3'	20.00	-19.00	excellent
hsa-miR-106b	NM_003150	428-455	3' UAGA-CGUGACAGUCGUGAAAU 5' 5' TCCTGGCATT----GCACTTTT 3'	25.00	-16.60	excellent
hsa-miR-106b	NM_003150	610-630	3' UAGACGUGACAGUCGUGAAAU 5' 5' GCCTGTAATCCCAGCACTTTG 3'	25.00	-23.50	excellent

Figure 3.11. Predictions for *STAT3* as a possible target of miR-106b. **A.** TargetScan predictions for miR-106b-*STAT3* interaction. Conserved and poorly conserved sites are shown. A more negative context score means higher prediction value. **B.** PITA predictions for miR-106b-*STAT3* interaction. A more negative ddG means higher prediction value. **C.** FindTar3 predictions for miR-106b-*STAT3* interaction. A more negative ΔG is associated with higher prediction value.

A

Conserved

	predicted consequential pairing of target region (top) and miRNA (bottom)	seed match	site-type contri-bution	3' pairing contribution	local AU contri-bution	position contri-bution	context+ score
Position 1142-1148 of AKT3 3' UTR hsa-miR-106b	5' ...GCUGAUGAGAAUCAUGCACUUUU... 3' UAGACGUGACAGUCGUGAAAU	7mer-m8	-0.120	0.012	-0.064	0.100	-0.03

B

Organism	Gene Name	microRNA	Position	Seed	dGduplex	dGopen	ddG	Conservation
Human	AKT3	hsa-miR-106b	1149	7:0:0	-14.01	-7.87	-6.13	1

C

miRNA	mRNA	Position	Structure	Loop Score	ΔG	Recommendation
hsa-miR-106b	NM_005465	245-267	3' UAGACGUGA--CAGUCG-UGAAAU 5' 5' GTCT-TACTATTATAGCAACTTTA 3'	25.00	-15.50	excellent
hsa-miR-106b	NM_005465	374-400	3' UAGACGUGAC----AGUCGUG--AAAU 5' 5' AGATACACTGATTCTAGGTACATTTTT 3'	20.00	-15.20	excellent
hsa-miR-106b	NM_005465	1118-1149	3' UAGACGUG----------ACAGUCGUGAAAU 5' 5' GATTGTACACGCTGATGAGAATCATGCACTTTT 3'	20.00	-20.50	excellent

Figure 3.12. Predictions for *AKT3* as a possible target of miR-106b. **A.** TargetScan predictions for miR-106b-*AKT3* interaction. Conserved sites are shown. A more negative context score means higher prediction value. **B.** PITA predictions for miR-106b-*AKT3* interaction. A more negative ddG means higher prediction value. **C.** FindTar3 predictions for miR-106b-*AKT3* interaction. A more negative ΔG value is associated with higher prediction value.

STAT3 is a transcription factor [145] and activate the transcription of EGF responsive genes, basically genes related with proliferation and motility. Down regulation of STAT3 by miR-106b and by turning off EGF pathway can both contribute a decrease in migration. AKT was shown to increase migration of MCF10A [141]. Therefore as in the case of STAT3, downregulation of AKT can lead to decrease migration of cells. Involvement of microRNAs in EGF signaling pathway regulation was shown in glioma [146], but miR-106b was not listed among those microRNAs. To understand the interaction between EGF and miR-106b, target candidates of miR-106b that have role in EGF pathway can be analyzed.

3.4.4 Matrigel Invasion Assay

To evaluate invasion abilities of MCF10A-EV and MCF10A-106b cells, matrigel invasion assay was performed. Matrigel mimics the basement membrane, so creating a suitable environment for invasion assays. Transwell inserts were covered with matrigel and pre-starved cells (in 1% serum, with EGF for MCF10A-EV and MCF10A-106b) were seeded onto the matrigel covered inserts. After 24 hours of incubation at 37 °C, invaded cells were counted. Representative images of invaded cells are shown in Figure 3.13.

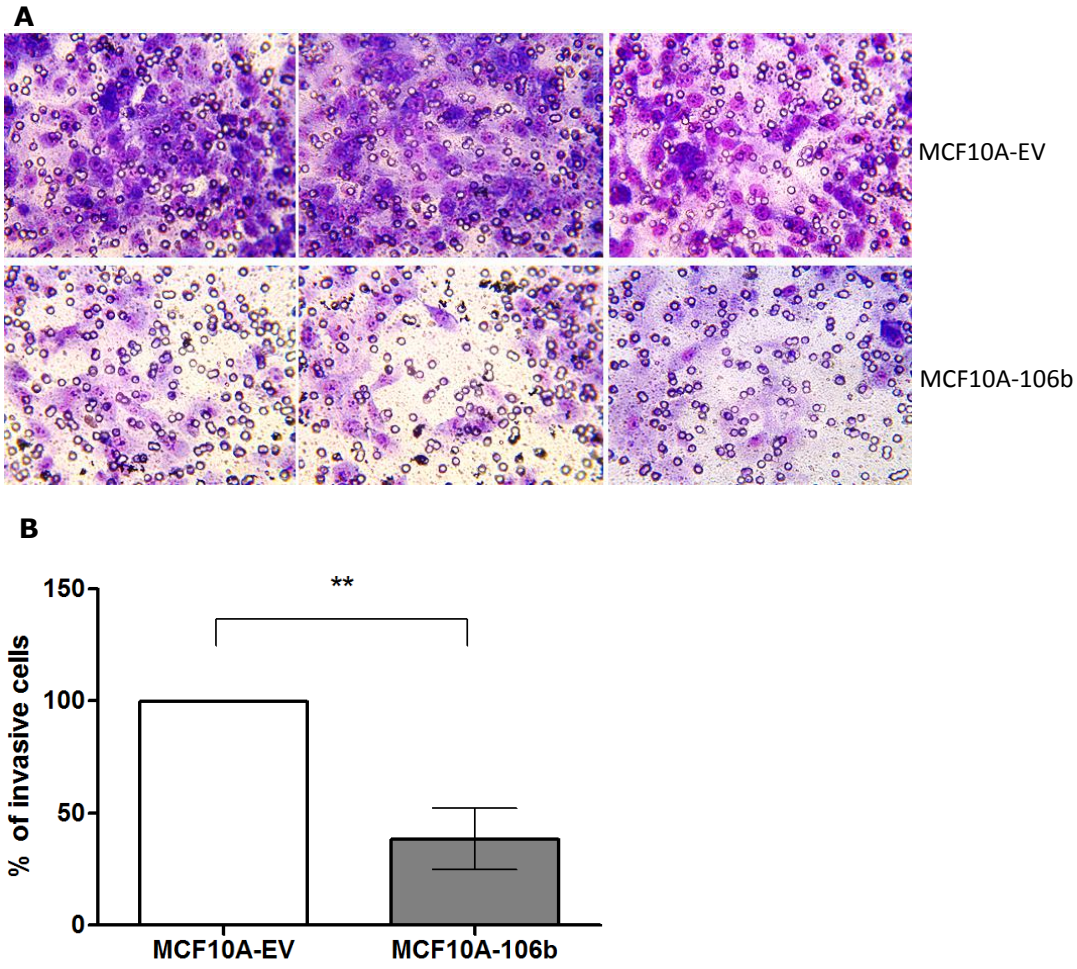

Figure 3.13. Matrigel invasion assay for MCF10A-EV and MCF10A-106b cells. **A.** Representative images of MCF10A-EV and MCF10A-106b cells invaded through membrane. Total magnification is 400X. **B.** Percentage of invaded cells through membrane at 24 hour. MCF10A-EV was set to 100%. Error bars represent the SD of three independent experiments with a total of six technical replicates. ** indicates significant difference between MCF10A-EV and MCF10A-106b $p<0.01$ (t test).

Based on experimental results (in the presence of EGF); migration of MCF10A-106b cells increased (Fig. 3.7) in contrast to invasion where MCF10A-106b cells invade 60% less compared to MCF10A-EV cells (Fig 3.11). This effect of miR-106b on MCF10A cells suggested involvement possible miR-106b targets that play role in invasion process. Given that MCF10A is a non-tumorigenic cell line, one would not expect a high invasive behavior [147]. Because we saw a significant decrease in MCF10A invasiveness due to miR-106b, we have also shown that the invasiveness of MCF10A cells were already low to begin with. MDA-MB-231 cells are known to be invasive and tumorigenic [148] and in our experimental system MDA-MB-231 cells were significantly more invasive than MCF10A cells (Figure 3.14).

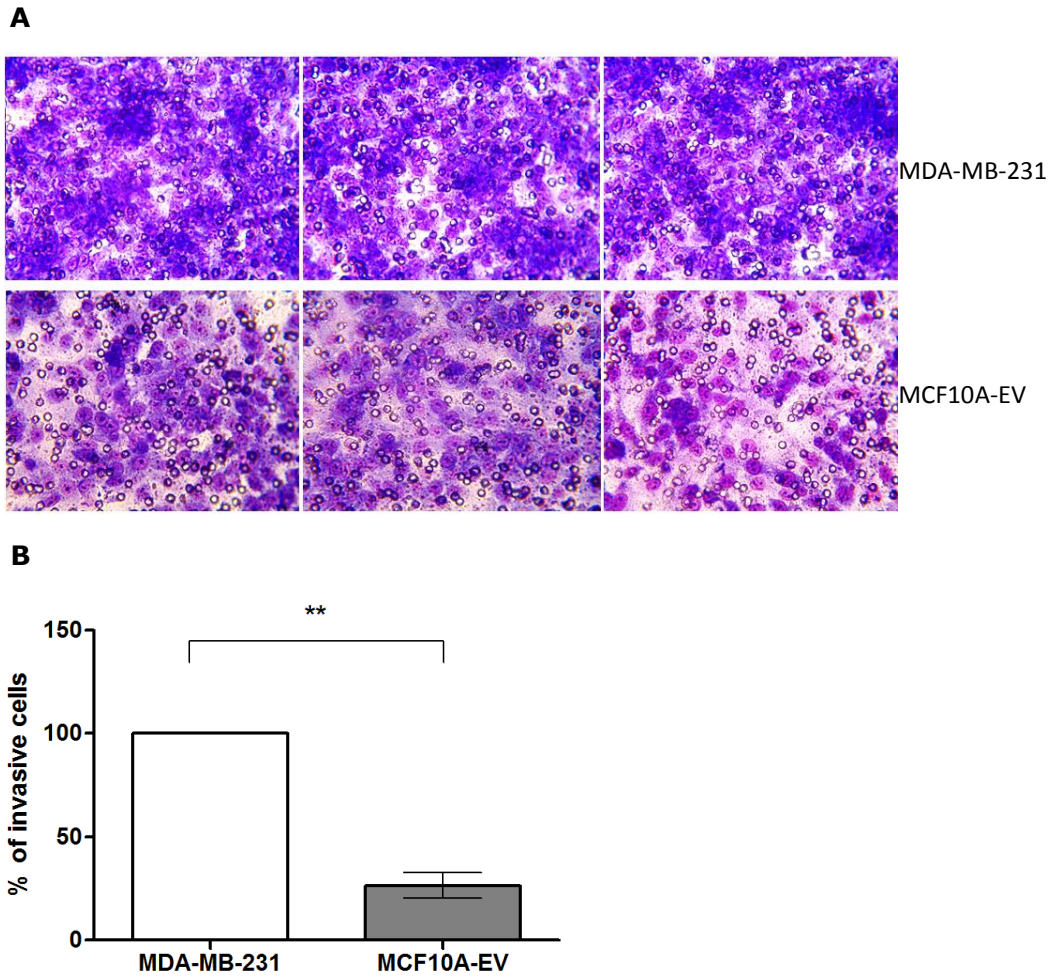

Figure 3.14. Matrigel invasion assay for MDA-MB-231 and MCF10A-EV cells. **A.** Representative images of MDA-MB-231 and MCF10A-EV cells invaded through membrane. Total magnification is 400X. **B.** Percentage of invaded cells through membrane at 24 hour. MDA-MB-231 was set to 100%. Error bar represents the SD of two independent experiments with a total of four technical replicates. ** indicates significant difference between MDA-MB-231 and MCF10A-EV $p<0.01$ (t test).

When different target prediction programs (TargetScan, FindTar3 and PITA) were scanned for predicted miR-106b targets, two proteins that might be important to explain the decrease in invasion ability of miR-106b expressing cells have arisen. Matrix metalloproteinase 2 (MMP2) [149] and matrix metalloproteinase 24 (MMP24) [150] are proteins involved in breaking down of extracellular matrix. These proteins are predicted targets of miR-106b based on different miRNA-mRNA target predictions program (TargetScan, PITA, FindTar3) (Figure 3.15 and Figure 3.16).

A

Conserved

	predicted consequential pairing of target region (top) and miRNA (bottom)	seed match	site-type contri-bution	3' pairing contri-bution	local AU contri-bution	position contri-bution	context+ score
Position 515-521 of MMP2 3' UTR hsa-miR-106b	5' ...CAGUUUGCUUUGUAUGCACUUUG... 3' UAGACGUGACAGUCGUGAAAU	7mer-m8	-0.120	0.003	-0.087	0.011	-0.15

Poorly Conserved

	predicted consequential pairing of target region (top) and miRNA (bottom)	seed match	site-type contri-bution	3' pairing contri-bution	local AU contri-bution	position contri-bution	context+ score
Position 1164-1170 of MMP2 3' UTR hsa-miR-106b	5' ...CUUUCUAUGUGCAAGGCACUUUU... 3' UAGACGUGACAGUCGUGAAAU	7mer-m8	-0.120	0.003	0.009	-0.053	-0.12

B

Organism	Gene Name	microRNA	Position	Seed	dGduplex	dGopen	ddG	Conservation
Human	MMP2	hsa-miR-106b	522	7:0:0	-18.4	-11.29	-7.1	0.24
Human	MMP2	hsa-miR-106b	1171	7:0:0	-15	-11.45	-3.54	0.00042

C

miRNA	mRNA	Position	Structure	Loop Score	ΔG	Recommendation
hsa-miR-106b	NM_001127891	502-522	3' UAGACGUGACAGUCGUGAAAU 5' :|:||*:||**||||||: 5' GTTTGCTTTGTATGCACTTTG 3'	20.00	-22.30	excellent
hsa-miR-106b	NM_001127891	1004-1024	3' UAGACGUGACAGUCG-UGAAAU-------- 5' **|||*****||||*|:|||:******** 5' CCCTGAAGAATCAGCAATTTTGTTGCTTTA 3'	15.00	-16.70	good
hsa-miR-106b	NM_001127891	1155-1171	3' UAGACGUGACAGUCGUGAAAU 5' ||*|||*****:||||||* 5' ATGTGCA----AGGCACTTTT 3'	20.00	-18.90	excellent

Figure 3.15. Predictions for *MMP2* as a possible target of miR-106b. **A.** TargetScan predictions for miR-106b-*MMP2* interaction. Conserved sites and poorly conserved sites are shown. A more negative context score means higher prediction value. **B.** PITA predictions for miR-106b-*MMP2* interaction. A more negative ddG means higher prediction value. **C.** FindTar3 predictions for miR-106b-*MMP2* interaction. A more negative ΔG is associated with higher prediction value.

A

Conserved

	predicted consequential pairing of target region (top) and miRNA (bottom)	seed match	site-type contri-bution	3' pairing contri-bution	local AU contri-bution	position contri-bution	context+ score
Position 1759-1766 of MMP24 3' UTR hsa-miR-106b	5' ...UUUAUACUUUGCAAAGCACUUUA... 3' UAGACGUGACAGUCGUGAAAU	8mer	-0.247	-0.008	-0.051	0.044	-0.19

B

Organism	Gene Name	microRNA	Position	Seed	dGduplex	dGopen	ddG	Conservation
Human	MMP24	hsa-miR-106b	1766	8:0:0	-17.11	-10.6	-6.5	1

C

miRNA	mRNA	Position	Structure	Loop Score	ΔG	Recommendation
hsa-miR-106b	NM_006690	694-713	3' UAGACGUGACAGUCGUGAAAU 5' 5' GTCACTACTGTC-CCATTTTG 3'	15.00	-17.20	good
hsa-miR-106b	NM_006690	1731-1754	3' UAGACGUG--ACAG-UCGUGAAAU 5' 5' GTTTGTACAGTGTTTTATACTTTG 3'	18.75	-17.50	good
hsa-miR-106b	NM_006690	1743-1766	3' UAGACGUGACAGUCGUGAAAU 5' 5' CTTTGCA----AAGCACTTTA 3'	20.00	-21.00	excellent
hsa-miR-106b	NM_006690	2288-2312	3' UAGACGUGAC---------AGUCGUGAAAU 5' 5' CTCAGC-CTGGGGGACATCACAGCATTTCA 3'	20.00	-20.00	excellent

Figure 3.16. Predictions for *MMP24* as a possible target of miR-106b. **A.** TargetScan predictions for miR-106b-*MMP24* interaction. Conserved sites are shown. A more negative context score means higher prediction value. **B.** PITA predictions for miR-106b-*MMP24* interaction. A more negative ddG means higher prediction value. **C.** FindTar3 predictions for miR-106b-*MMP24* interaction. A more negative ΔG value is associated with higher prediction value.

MMP2 itself plays role in digestion of matrix, whereas MMP24 activates MMP2. If miR-106b targets and decrease the protein level of MMP2 invasion ability of these cells might decrease as we have observed in matrigel invasion assay (Figure 3.13).

Based on these functional assays, effect of miR-106b in MCF10A cells were observed in different respects: proliferation, motility, migration and invasion. miR-106b expression, resulted in an increase proliferation rate , motility and migration of MCF10A cells. However, miR-106b overexpression caused a reduction in the invasion ability of MCF10A cells.

As stated in introduction chapter, miR-106b belongs to a microRNA cluster which contains two other members (miR-93 and miR-25). These three microRNAs are transcribed from the 13th intron of same gene, minichromosome maintenance complex component 7 (MCM7). Transcription regulations of these microRNAs follow the same pattern of *MCM7* transcript [115] controlled by E2F1 transcription factor. Therefore to better understand the role of miR-106b, other members of cluster should also be considered. miR-93

and miR-106b have same seed sequence and have shared mRNA targets (TargetScan, PITA, PicTar, FindTar3). Having some common targets, miR-93 and miR-106b might possibly work in a coordinated manner with each other. Overexpressing the entire cluster might be another approach to investigate the role of these microRNAs.

CHAPTER 4

CONCLUSION

The aim of this study was to investigate the role of miR-106b in breast cancer. As a continuation of previous experiments performed by Dr. Ayşegül Sapmaz, in our laboratory, phenotypical analysis of MCF10A cells that stably overexpress miR-106b was performed.

Ectopic expression of miR-106b in MCF10A cells caused a 57% increase in proliferation rate. In *in vitro* wound healing and transwell migration assays it was observed that miR-106b caused an increase in the migration ability of MCF10A cells when they were grown in complete growth medium. In contrast to increase in the migration ability of MCF10A cells upon miR-106b expression, invasion ability decreased. Although it is an interesting finding, it needs further investigations such as target confirmation to explain the observed phenotype in MCF10A-106b cells.

Depending on our results, migration and invasion pathways were affected differently when miR-106b was overexpressed. These two processes have different properties. In invasion, cells need to degrade a basement membrane by the aid of proteases. Migration, on the other hand, requires reorganization of cytoskeletal elements. Therefore, different regulation of migration and invasion in the presence of miR-106b can be explained by mRNAs targeted by miR-106b. Further studies such as investigation of some possible targets are needed to elucidate pathways that miR-106b involved in.

Interestingly a possible relation between miR-106b and EGF was suggested depending on our results. Although this finding is so immature to lead us a conclusion, common proteins in both EGF pathway and miR-106b pathway might imply a communication between those pathways. Further studies are planned to analyze EGF-miR-106b relation.

Based on our data, contributions of miR-106b on transformation of MCF10A cells might be inferred. miR-106b overexpression resulted in an increase proliferation, motility and migration and a decrease in invasion. To elucidate these phenotypical effects of miR-106b, future studies are needed to understand targets of miR-106b that regulate proliferation, migration, invasion and others that plays role in tumorigenesis.

REFERENCES

(1) Lee, R. C.; Feinbaum, R. L.; Ambros, V. The C. elegans heterochronic gene lin-4 encodes small RNAs with antisense complementarity to lin-14. *Cell* **1993**, *75*, 843–54.

(2) Elbashir, S. M.; Lendeckel, W.; Tuschl, T. RNA interference is mediated by 21- and 22-nucleotide RNAs. *Genes and Development* **2001**, *15*, 188–200.

(3) Lagos-Quintana, M.; Rauhut, R.; Lendeckel, W.; Tuschl, T. Identification of novel genes coding for small expressed RNAs. *Science* **2001**, *294*, 853–8.

(4) Llave, C.; Kasschau, K. D.; Rector, M. A.; Carrington, J. C. Endogenous and Silencing-Associated Small RNAs in Plants. *The Plant Cell* **2002**, *14*, 1605–1619.

(5) Pfeffer, S.; Zavolan, M.; Grässer, F. a; Chien, M.; Russo, J. J.; Ju, J.; John, B.; Enright, A. J.; Marks, D.; Sander, C.; Tuschl, T. Identification of virus-encoded microRNAs. *Science* **2004**, *304*, 734–6.

(6) Kozomara, A.; Griffiths-Jones, S. miRBase: integrating microRNA annotation and deep-sequencing data. *Nucleic acids research* **2011**, *39*, D152–7.

(7) Floyd, K. S.; Bowman, L. J. Ancient microRNA target sequences in plants. *Nature* **2004**, *428*, 485–486.

(8) Bartel, D. P.; Lee, R.; Feinbaum, R. MicroRNAs : Genomics , Biogenesis , Mechanism , and Function Genomics : The miRNA Genes. *Cell* **2004**, *116*, 281–297.

(9) Lee, Y.; Kim, M.; Han, J.; Yeom, K.-H.; Lee, S.; Baek, S. H.; Kim, V. N. MicroRNA genes are transcribed by RNA polymerase II. *The EMBO journal* **2004**, *23*, 4051–60.

(10) Winter, J.; Jung, S.; Keller, S.; Gregory, R. I.; Diederichs, S. Many roads to maturity: microRNA biogenesis pathways and their regulation. *Nature Cell Biology* **2009**, *11*, 228–34.

(11) Borchert, G. M.; Lanier, W.; Davidson, B. L. RNA polymerase III transcribes human microRNAs. *Nature Structural & Molecular Biology* **2006**, *13*, 1097–101.

(12) Canella, D.; Praz, V.; Reina, J. H.; Cousin, P.; Hernandez, N. Defining the RNA polymerase III transcriptome : Genome-wide localization of the RNA polymerase III transcription machinery in human cells. *Genome research* **2010**, *20*, 710–721.

(13) Lee, Y.; Ahn, C.; Han, J.; Choi, H.; Kim, J.; Yim, J.; Lee, J.; Provost, P.; Rådmark, O.; Kim, S.; Kim, V. N. The nuclear RNase III Drosha initiates microRNA processing. *Nature* **2003**, *425*, 415–419.

(14) Denli, A. M.; Tops, B. B. J.; Plasterk, R. H. A.; Ketting, R. F.; Hannon, G. J. Processing of primary microRNAs by the Microprocessor complex. *Nature* **2004**, *432*, 231–235.

(15) Gregory, R. I.; Yan, K.; Amuthan, G.; Chendrimada, T.; Doratotaj, B.; Cooch, N.; Shiekhattar, R. The Microprocessor complex mediates the genesis of microRNAs. *Nature* **2004**, *432*, 235–240.

(16) Han, J.; Lee, Y.; Yeom, K. H.; Kim, Y. K.; Jin, H.; Kim, V. N. The Drosha-DGCR8 complex in primary microRNA processing. *Genes & Development* **2004**, *18*, 3016–27.
(17) Kim, V. N. MicroRNA biogenesis: coordinated cropping and dicing. *Nature Reviews. Molecular Cell Biology* **2005**, *6*, 376–85.
(18) Wu, H.; Xu, H.; Miraglia, L. J.; Crooke, S. T. Human RNase III is a 160-kDa protein involved in preribosomal RNA processing. *The Journal of Biological Chemistry* **2000**, *275*, 36957–65.
(19) Zeng, Y.; Cullen, B. R. Sequence requirements for micro RNA processing and function in human cells. *RNA* **2003**, *9*, 112–123.
(20) Han, J.; Lee, Y.; Yeom, K. H.; Nam, J. W.; Heo, I.; Rhee, J. K.; Sohn, S. Y.; Cho, Y.; Zhang, B.- ak; Kim, V. N. Molecular basis for the recognition of primary microRNAs by the Drosha-DGCR8 complex. *Cell* **2006**, *125*, 887–901.
(21) Yi, R.; Qin, Y.; Macara, I. G.; Cullen, B. R. Exportin-5 mediates the nuclear export of pre-microRNAs and short hairpin RNAs. *Genes & Development* **2003**, *17*, 3011–3016.
(22) Ketting, R. F.; Fischer, S. E. J.; Bernstein, E.; Sijen, T.; Hannon, G. J.; Plasterk, R. H. A. Dicer functions in RNA interference and in synthesis of small RNA involved in developmental timing in C . elegans. *Genes & Development* **2001**, *15*, 2654–2659.
(23) Knight, S. W.; Bass, B. L. A role for the RNase III enzyme DCR-1 in RNA interference and germ line development in Caenorhabditis elegans. *Science* **2001**, *293*, 2269–71.
(24) Ma, J. B.; Ye, K.; Patel, D. J. Structural basis for overhang-specific small interfering RNA recognition by the PAZ domain. *Nature* **2004**, *429*, 318–322.
(25) Tsutsumi, A.; Kawamata, T.; Izumi, Natsuko Seitz, H.; Tomari, Y. Recognition of the pre-miRNA structure by Drosophila Dicer-1. *Nature Structural & Molecular Biology* **2011**, *18*, 1153–1158.
(26) Gregory, R. I.; Chendrimada, T. P.; Cooch, N.; Shiekhattar, R. Human RISC couples microRNA biogenesis and posttranscriptional gene silencing. *Cell* **2005**, *123*, 631–40.
(27) Schwarz, D. S.; Hutvágner, G.; Du, T.; Xu, Z.; Aronin, N.; Zamore, P. D. Asymmetry in the assembly of the RNAi enzyme complex. *Cell* **2003**, *115*, 199–208.
(28) Khvorova, A.; Reynolds, A.; Jayasena, S. D. Functional siRNAs and miRNAs exhibit strand bias. *Cell* **2003**, *115*, 209–16.
(29) Ro, S.; Park, C.; Young, D.; Sanders, K. M.; Yan, W. Tissue-dependent paired expression of miRNAs. *Nucleic Acids Research* **2007**, *35*, 5944–53.
(30) Garzon, R.; Calin, G. a; Croce, C. M. MicroRNAs in Cancer. *Annual Review of Medicine* **2009**, *60*, 167–79.
(31) Ruby, J. G.; Jan, C. H.; Bartel, D. P. Intronic microRNA precursors that bypass Drosha processing. *Nature* **2007**, *448*, 83–86.
(32) Jan, C.; Friedman, R.; Ruby, J.; Bartel, D. Formation, regulation and evolution of Caenorhabditis elegans 3'UTRs. *Nature* **2011**, *469*, 97–101.
(33) Westholm, J. O.; Lai, E. C. Mirtrons: microRNA biogenesis via splicing. *Biochimie* **2011**, *93*, 1897–904.

(34) Berezikov, E.; Chung, W. J.; Willis, J.; Cuppen, E.; Lai, E. C. Mammalian Mirtron Genes. *Molecular Cell* **2007**, *28*, 328–336.
(35) Sibley, C. R.; Seow, Y.; Saayman, S.; Dijkstra, K. K.; El Andaloussi, S.; Weinberg, M. S.; Wood, M. J. a The biogenesis and characterization of mammalian microRNAs of mirtron origin. *Nucleic Acids Research* **2011**, *40*, 438–48.
(36) Naqvi, A. R.; Islam, M. N.; Choudhury, N. R.; Rizwanul Haq., Q. M. The Fascinating World of RNA Interference. *International Journal of Biological Sciences* **2009**, *5*, 97–117.
(37) Friedman, R. C.; Farh, K. K.; Burge, C. B.; Bartel, D. P. Most mammalian mRNAs are conserved targets of microRNAs. *Genome Research* **2009**, *19*, 92–105.
(38) Nilsen, T. W. Mechanisms of microRNA-mediated gene regulation in animal cells. *Trends in Genetics* **2007**, *23*, 243–9.
(39) Zhanga, R.; Su, B. Small but influential: the role of microRNAs on gene regulatory network and 3'UTR evolution. *Journal of Genetics and Genomics* **2009**, *36*, 1–6.
(40) Lee, I.; Ajay, S. S.; Yook, J. I.; Kim, H. S.; Hong, S. H.; Kim, N. H.; Dhanasekaran, S. M.; Chinnaiyan, A. M.; Athey, B. D. New class of microRNA targets containing simultaneous 5'-UTR and 3 '-UTR interaction sites. *Genome Research* **2009**, *19*, 1175–1183.
(41) Ørom, U. A.; Nielsen, F. C.; Lund, A. H. MicroRNA-10a binds the 5'UTR of ribosomal protein mRNAs and enhances their translation. *Molecular Cell* **2008**, *30*, 460–71.
(42) He, L.; Hannon, G. J. MicroRNAs: small RNAs with a big role in gene regulation. *Nature Reviews. Genetics* **2004**, *5*, 522–31.
(43) Axtell, M. J.; Westholm, J. O.; Lai, E. C. Vive la différence: biogenesis and evolution of microRNAs in plants and animals. *Genome Biology* **2011**, *12*, 221.
(44) Brodersen, P.; Achard, Lali Sakvarelidze Rasmussen, M. B.; Dunoyer, P.; Yamamoto, Y. Y.; Sieburth, L.; Voinnet, O. Widespread Translational Inhibition by Plant miRNAs and siRNAs. *Science* **2008**, *320*, 1185–1190.
(45) Kawasaki, H.; Taira, K. MicroRNA-196 inhibits HOXB8 expression in myeloid differentiation of HL60 cells. *Nucleic Acids Symposium Series* **2004**, *48*, 211–2.
(46) Yu, Z.; Raabe, T.; Hecht, N. B. MicroRNA Mirn122a reduces expression of the posttranscriptionally regulated germ cell transition protein 2 (Tnp2) messenger RNA (mRNA) by mRNA cleavage. *Biology of Reproduction* **2005**, *73*, 427–33.
(47) Doench, J. G.; Sharp, P. A. Specificity of microRNA target selection in translational repression. *Genes & Development* **2004**, *18*, 504–11.
(48) Grimson, A.; Farh, K. K.-H.; Johnston, W. K.; Garrett-Engele, P.; Lim, L. P.; Bartel, D. P. MicroRNA targeting specificity in mammals: determinants beyond seed pairing. *Molecular cell* **2007**, *27*, 91–105.
(49) Bartel, D. P. MicroRNAs: target recognition and regulatory functions. *Cell* **2009**, *136*, 215–33.
(50) Lewis, B. P.; Burge, C. B.; Bartel, D. P. Conserved seed pairing, often flanked by adenosines, indicates that thousands of human genes are microRNA targets. *Cell* **2005**, *120*, 15–20.

(51) Garcia, D. M.; Baek, D.; Shin, C.; Bell, G. W.; Grimson, A.; Bartel, D. P. Weak seed-pairing stability and high target-site abundance decrease the proficiency of lsy-6 and other microRNAs. *Nature Structural & Molecular Biology* **2011**, *18*, 1139–1146.
(52) Kertesz, M.; Iovino, N.; Unnerstall, U.; Gaul, U.; Segal, E. The role of site accessibility in microRNA target recognition. *Nature Genetics* **2007**, *39*, 1278–84.
(53) Krek, A.; Grün, D.; Poy, M. N.; Wolf, R.; Rosenberg, L.; Epstein, E. J.; MacMenamin, P.; da Piedade, I.; Gunsalus, K. C.; Stoffel, M.; Rajewsky, N. Combinatorial microRNA target predictions. *Nature Genetics* **2005**, *37*, 495–500.
(54) Ye, W.; Lv, Q.; Wong, C.-K. A.; Hu, S.; Fu, C.; Hua, Z.; Cai, G.; Li, G.; Yang, B. B.; Zhang, Y. The effect of central loops in miRNA:MRE duplexes on the efficiency of miRNA-mediated gene regulation. *PloS one* **2008**, *3*, e1719.
(55) Ameres, S. L.; Horwich, M. D.; Hung, J.-H.; Xu, J.; Ghildiyal, M.; Weng, Z.; Zamore, P. D. Target RNA-directed trimming and tailing of small silencing RNAs. *Science* **2010**, *328*, 1534–9.
(56) Hawkins, P.; Morris, K. V. RNA and transcriptional modulation of gene expression. *Cell Cycle* **2008**, *7*, 602–607.
(57) Bayne, E. H.; Allshire, R. C. RNA-directed transcriptional gene silencing in mammals. *TRENDS in Genetics* **2005**, *21*, 370–373.
(58) Kim, D. H.; Saetrom, P.; Snøve, O.; Rossi, J. J. MicroRNA-directed transcriptional gene silencing in mammalian cells. *Proceedings of the National Academy of Sciences of the United States of America* **2008**, *105*, 16230–5.
(59) Tan, Y.; Zhang, B.; Wu, T.; Skogerbø, G.; Zhu, X.; Guo, X.; He, S.; Chen, R. Transcriptional inhibiton of Hoxd4 expression by miRNA-10a in human breast cancer cells. *BMC Molecular Biology* **2009**, *10*, 12.
(60) Calin, G. A.; Dumitru, C. D.; Shimizu, M.; Bichi, R.; Zupo, S.; Noch, E.; Aldler, H.; Rattan, S.; Keating, M.; Rai, K.; Rassenti, L.; Kipps, T.; Negrini, M.; Bullrich, F.; Croce, C. M. Frequent deletions and down-regulation of micro- RNA genes miR15 and miR16 at 13q14 in chronic lymphocytic leukemia. *Proceedings of the National Academy of Sciences of the United States of America* **2002**, *99*, 15524–9.
(61) Cimmino, A.; Calin, G. A.; Fabbri, M.; Iorio, M. V.; Ferracin, M.; Shimizu, M.; Wojcik, S. E.; Aqeilan, R. I.; Zupo, S.; Dono, M.; Rassenti, L.; Alder, H.; Volinia, S.; Liu, C.-G.; Kipps, T. J.; Negrini, M.; Croce, C. M. miR-15 and miR-16 induce apoptosis by targeting BCL2. *Proceedings of the National Academy of Sciences of the United States of America* **2005**, *102*, 13944–9.
(62) Calin, G. A.; Sevignani, C.; Dumitru, C. D.; Hyslop, T.; Noch, E.; Yendamuri, S.; Shimizu, M.; Rattan, S.; Bullrich, F.; Negrini, M.; Croce, C. M. Human microRNA genes are frequently located at fragile sites and genomic regions involved in cancers. *Proceedings of the National Academy of Sciences of the United States of America* **2004**, *101*, 2999–3004.
(63) Laganà, A.; Russo, F.; Sismeiro, C.; Giugno, R.; Pulvirenti, A.; Ferro, A. Variability in the incidence of miRNAs and genes in fragile sites and the role of repeats and CpG islands in the distribution of genetic material. *PloS one* **2010**, *5*, e11166.

(64) Iorio, M. V.; Croce, C. M. microRNA involvement in human cancer. *Carcinogenesis* **2012**, *33*, 1126–33.
(65) Lu, J.; Getz, G.; Miska, E. A.; Alvarez-Saavedra, E.; Lamb, J.; Peck, D.; Sweet-Cordero, A.; Ebert, B. L.; Mak, R. H.; Ferrando, A. A.; Downing, J. R.; Jacks, T.; Horvitz, H. R.; Golub, T. R. MicroRNA expression profiles classify human cancers. *Nature* **2005**, *475*, 834–838.
(66) Farazi, T. a; Horlings, H. M.; Ten Hoeve, J. J.; Mihailovic, A.; Halfwerk, H.; Morozov, P.; Brown, M.; Hafner, M.; Reyal, F.; van Kouwenhove, M.; Kreike, B.; Sie, D.; Hovestadt, V.; Wessels, L. F. a; van de Vijver, M. J.; Tuschl, T. MicroRNA sequence and expression analysis in breast tumors by deep sequencing. *Cancer Research* **2011**, *71*, 4443–53.
(67) Sempere, L. F.; Christensen, M.; Silahtaroglu, A.; Bak, M.; Heath, C. V.; Schwartz, G.; Wells, W.; Kauppinen, S.; Cole, C. N. Altered MicroRNA expression confined to specific epithelial cell subpopulations in breast cancer. *Cancer Research* **2007**, *67*, 11612–20.
(68) Lowery, A. J.; Miller, N.; Devaney, A.; McNeill, R. E.; Davoren, P. a; Lemetre, C.; Benes, V.; Schmidt, S.; Blake, J.; Ball, G.; Kerin, M. J. MicroRNA signatures predict oestrogen receptor, progesterone receptor and HER2/neu receptor status in breast cancer. *Breast Cancer Research* **2009**, *11*, R27.
(69) Lim, L. P.; Lau, N. C.; Garrett-Engele, P.; Grimson, A.; Schelter, J. M.; Castle, J.; Bartel, D. P.; Linsley, P. S.; Johnson, J. M. Microarray analysis shows that some microRNAs downregulate large numbers of target mRNAs. *Nature* **2005**, *433*, 769–773.
(70) Hanahan, D.; Weinberg, R. a Hallmarks of cancer: the next generation. *Cell* **2011**, *144*, 646–74.
(71) Weber, B.; Stresemann, C.; Brueckner, B.; Lyko, F. Methylation of human microRNA genes in normal and neoplastic cells. *Cell Cycle* **2007**, *6*, 1001–5.
(72) Lehmann, U.; Hasemeier, B.; Christgen, M.; Müller, M.; Römermann, D.; Länger, F.; Kreipe, H. Epigenetic inactivation of microRNA gene hsa-mir-9-1 in human breast cancer. *The Journal of Pathology* **2008**, *214*, 17–24.
(73) Lujambio, A.; Esteller, M. CpG Island Hypermethylation of Tumor Suppressor microRNAs in Human Cancer. *Cell Cycle* **2007**, *6*, 1455–1459.
(74) Scott, G. K.; Mattie, M. D.; Berger, C. E.; Benz, S. C.; Benz, C. C. Rapid alteration of microRNA levels by histone deacetylase inhibition. *Cancer Research* **2006**, *66*, 1277–81.
(75) Saito, Y.; Liang, G.; Egger, G.; Friedman, J. M.; Chuang, J. C.; Coetzee, G. A.; Jones, P. A. Specific activation of microRNA-127 with downregulation of the proto-oncogene BCL6 by chromatin-modifying drugs in human cancer cells. *Cancer Cell* **2006**, *9*, 435–443.
(76) Chang, T.-C.; Wentzel, E. a; Kent, O. a; Ramachandran, K.; Mullendore, M.; Lee, K. H.; Feldmann, G.; Yamakuchi, M.; Ferlito, M.; Lowenstein, C. J.; Arking, D. E.; Beer, M. a; Maitra, A.; Mendell, J. T. Transactivation of miR-34a by p53 broadly influences gene expression and promotes apoptosis. *Molecular Cell* **2007**, *26*, 745–52.

(77) Bommer, G. T.; Gerin, I.; Feng, Y.; Kaczorowski, A. J.; Kuick, R.; Love, R. E.; Zhai, Y.; Giordano, T. J.; Qin, Z. S.; Moore, B. B.; MacDougald, O. a; Cho, K. R.; Fearon, E. R. p53-mediated activation of miRNA34 candidate tumor-suppressor genes. *Current Biology* **2007**, *17*, 1298–307.
(78) O'Donnell, K. A.; Wentze, E. A.; Zeller, K. I.; Dang, C. V.; Mendell, J. T. c-Myc-regulated microRNAs modulate E2F1 expression. *Nature* **2005**, *435*, 839–843.
(79) Garzon, R.; Fabbri, M.; Cimmino, A.; Calin, G. a; Croce, C. M. MicroRNA expression and function in cancer. *Trends in Molecular Medicine* **2006**, *12*, 580–7.
(80) Yanaihara, N.; Caplen, N.; Bowman, E.; Seike, M.; Kumamoto, K.; Yi, M.; Stephens, R.; Okamoto, A.; Yokota, J.; Tanaka, T.; Calin, G.; Liu, C.; Croce, C.; Harris, C. Unique microRNA molecular profiles in lung cancer diagnosis and prognosis. *Cancer Cell* **2006**, *9*, 189–198.
(81) Iorio, M. V.; Ferracin, M.; Liu, C.-G.; Veronese, A.; Spizzo, R.; Sabbioni, S.; Magri, E.; Pedriali, M.; Fabbri, M.; Campiglio, M.; Ménard, S.; Palazzo, J. P.; Rosenberg, A.; Musiani, P.; Volinia, S.; Nenci, I.; Calin, G. a; Querzoli, P.; Negrini, M.; Croce, C. M. MicroRNA gene expression deregulation in human breast cancer. *Cancer Research* **2005**, *65*, 7065–70.
(82) Johnson, S. M.; Grosshans, H.; Shingara, J.; Byrom, M.; Jarvis, R.; Cheng, A.; Labourier, E.; Reinert, K. L.; Brown, D.; Slack, F. J. RAS is regulated by the let-7 microRNA family. *Cell* **2005**, *120*, 635–47.
(83) Scott, G. K.; Goga, A.; Bhaumik, D.; Berger, C. E.; Sullivan, C. S.; Benz, C. C. Coordinate suppression of ERBB2 and ERBB3 by enforced expression of micro-RNA miR-125a or miR-125b. *The Journal of Biological Chemistry* **2007**, *282*, 1479–86.
(84) Akhavantabasi, S.; Sapmaz, A.; Tuna, S.; Erson-Bensan, A. E. miR-125b targets ARID3B in breast cancer cells. *Cell Structure and Function* **2012**, *37*, 27–38.
(85) Metzler, M.; Wilda, M.; Busch, K.; Viehmann, S.; Borkhardt, A. High expression of precursor microRNA-155/BIC RNA in children with Burkitt lymphoma. *Genes Chromosomes and Cancer* **2004**, *39*, 167–169.
(86) Calin, G. A.; Ferracin, M.; Cimmino, A.; Di Leva, G.; Shimizu, M.; Wojcik, S. E.; Iorio, M. V.; Visone, R.; Sever, N. I.; Fabbri, M.; Iuliano, R.; Palumbo, T.; Pichiorri, F.; Roldo, C.; Garzon, R.; Sevignani, C.; Rassenti, L.; Alder, H.; Volinia, S.; Liu, C.; Kipps, T. J.; Negrini, M.; Croce, C. M. A MicroRNA signature associated with prognosis and progression in chronic lymphocytic leukemia. *The New England Journal of Medicine* **2005**, *353*, 1793–801.
(87) Garzon, R.; Volinia, S.; Liu, C.-G.; Fernandez-Cymering, C.; Palumbo, T.; Pichiorri, F.; Fabbri, M.; Coombes, K.; Alder, H.; Nakamura, T.; Flomenberg, N.; Marcucci, G.; Calin, G. a; Kornblau, S. M.; Kantarjian, H.; Bloomfield, C. D.; Andreeff, M.; Croce, C. M. MicroRNA signatures associated with cytogenetics and prognosis in acute myeloid leukemia. *Blood* **2008**, *111*, 3183–9.
(88) Neilsen, P.; Noll, J.; Mattiske, S.; Bracken, C.; Gregory, P.; Schulz, R.; Lim, S.; Kumar, R.; Suetani, R.; Goodall, G.; Callen, D. Mutant p53 drives invasion in breast tumors through up-regulation of miR-155. *Oncogene* **2012**.

(89) Ciafrè, S.; Galardi, S.; Mangiola, A.; Ferracin, M.; Liu, C.; Sabatino, G.; Negrini, M.; Maira, G.; Croce, C.; Farace, M. Extensive modulation of a set of microRNAs in primary glioblastoma. *Biochemical and Biophysical Research Communications* **2005**, *334*, 1351–1358.
(90) Volinia, S.; Calin, G. a; Liu, C.-G.; Ambs, S.; Cimmino, A.; Petrocca, F.; Visone, R.; Iorio, M.; Roldo, C.; Ferracin, M.; Prueitt, R. L.; Yanaihara, N.; Lanza, G.; Scarpa, A.; Vecchione, A.; Negrini, M.; Harris, C. C.; Croce, C. M. A microRNA expression signature of human solid tumors defines cancer gene targets. *Proceedings of the National Academy of Sciences of the United States of America* **2006**, *103*, 2257–61.
(91) Meng, F.; Henson, R.; Wehbe–Janek, H.; Ghoshal, K.; Jacob, S. T.; Tushar, P. MicroRNA-21 Regulates Expression of the PTEN Tumor Suppressor Gene in Human Hepatocellular Cancer. *Gastroenterology* **2007**, *133*, 647–658.
(92) Frankel, L. B.; Christoffersen, N. R.; Jacobsen, A.; Lindow, M.; Krogh, A.; Lund, A. H. Programmed cell death 4 (PDCD4) is an important functional target of the microRNA miR-21 in breast cancer cells. *The Journal of Biological Chemistry* **2008**, *283*, 1026–33.
(93) Zhu, S.; Si, M.-L.; Wu, H.; Mo, Y.-Y. MicroRNA-21 targets the tumor suppressor gene tropomyosin 1 (TPM1). *The Journal of Biological Chemistry* **2007**, *282*, 14328–36.
(94) Mendell, J. T. miRiad roles for the miR-17-92 cluster in development and disease. *Cell* **2008**, *133*, 217–22.
(95) Leone, G.; DeGregori, J.; Sears, R.; Jakoi, L.; Nevins, J. R. Myc and Ras collaborate in inducing accumulation of active cyclin E/Cdk2 and E2F. *Nature* **1997**, *387*, 422–426.
(96) Xiang, J.; Wu, J. Feud or Friend? The Role of the miR-17-92 Cluster in Tumorigenesis. *Current Genomics* **2010**, *11*, 129–135.
(97) Linsley, P. S.; Schelter, J.; Burchard, J.; Kibukawa, M.; Martin, M. M.; Bartz, S. R.; Johnson, J. M.; Cummins, J. M.; Raymond, C. K.; Dai, H.; Chau, N.; Cleary, M.; Jackson, A. L.; Carleton, M.; Lim, L. Transcripts targeted by the microRNA-16 family cooperatively regulate cell cycle progression. *Molecular and Cellular Biology* **2007**, *27*, 2240–52.
(98) Bonci, D.; Coppola, V.; Musumeci, M.; Addario, A.; Giuffrida, R.; Memeo, L.; D'Urso, L.; Pagliuca, A.; Biffoni, M.; Labbaye, C.; Bartucci, M.; Muto, G.; Peschle, C.; De Maria, R. The miR-15a-miR-16-1 cluster controls prostate cancer by targeting multiple oncogenic activities. *Nature Medicine* **2008**, *14*, 1271–1277.
(99) Ventura, A.; Young, A. G.; Winslow, M. M.; Lintault, L.; Meissner, A.; Erkeland, S. J.; Newman, J.; Bronson, R. T.; Crowley, D.; Stone, J. R.; Jaenisch, R.; Sharp, P. a; Jacks, T. Targeted deletion reveals essential and overlapping functions of the miR-17 -92 family of miRNA clusters. *Cell* **2008**, *132*, 875–86.
(100) Lee, Y. S.; Dutta, A. The tumor suppressor microRNA let-7 represses the HMGA2 oncogene. *Genes & Development* **2007**, *21*, 1025–30.
(101) Mott, J. L.; Kobayashi, S.; Bronk, S. F.; Gores, G. J. mir-29 regulates Mcl-1 protein expression and apoptosis. *Oncogene* **2007**, *26*, 6133–40.

(102) Fabbri, M.; Garzon, R.; Cimmino, A.; Liu, Z.; Zanesi, N.; Callegari, E.; Liu, S.; Alder, H.; Costinean, S.; Fernandez-Cymering, C.; Volinia, S.; Guler, G.; Morrison, C. D.; Chan, K. K.; Marcucci, G.; Calin, G. a; Huebner, K.; Croce, C. M. MicroRNA-29 family reverts aberrant methylation in lung cancer by targeting DNA methyltransferases 3A and 3B. *Proceedings of the National Academy of Sciences of the United States of America* **2007**, *104*, 15805–10.
(103) Voorhoeve, P. M.; le Sage, C.; Schrier, M.; Gillis, A. J. M.; Stoop, H.; Nagel, R.; Liu, Y.-P.; van Duijse, J.; Drost, J.; Griekspoor, A.; Zlotorynski, E.; Yabuta, N.; De Vita, G.; Nojima, H.; Looijenga, L. H. J.; Agami, R. A genetic screen implicates miRNA-372 and miRNA-373 as oncogenes in testicular germ cell tumors. *Cell* **2006**, *124*, 1169–81.
(104) Raver-Shapira, N.; Marciano, E.; Meiri, E.; Spector, Y.; Rosenfeld, N.; Moskovits, N.; Bentwich, Z.; Oren, M. Transcriptional activation of miR-34a contributes to p53-mediated apoptosis. *Molecular Cell* **2007**, *26*, 731–43.
(105) Metzler, M.; Wilda, M.; Busch, K.; Viehmann, S.; Borkhardt, A. High expression of precursor microRNA-155/BIC RNA in children with Burkitt lymphoma. *Genes Chromosomes and Cancer* **2004**, *39*, 167–169.
(106) Kluiver, J.; Poppemas, S.; de Jong, D.; Blokzijl, T.; Harms, G.; Jacobs, S.; Kroesen, B.; van den Berg, A. BIC and miR-155 are highly expressed in Hodgkin, primary mediastinal and diffuse large B cell lymphomas. *The Journal of Pathology* **2005**, *207*, 243–249.
(107) Ma, L. Role of miR-10b in breast cancer metastasis. *Breast Cancer Research* **2010**, *12*, 210.
(108) Ivanovska, I.; Ball, A. S.; Diaz, R. L.; Magnus, J. F.; Kibukawa, M.; Schelter, J. M.; Kobayashi, S. V.; Lim, L.; Burchard, J.; Jackson, A. L.; Linsley, P. S.; Cleary, M. a MicroRNAs in the miR-106b family regulate p21/CDKN1A and promote cell cycle progression. *Molecular and Cellular Biology* **2008**, *28*, 2167–74.
(109) Li, Y.; Tan, W.; Neo, T. W. L.; Aung, M. O.; Wasser, S.; Lim, S. G.; Tan, T. M. C. Role of the miR-106b-25 microRNA cluster in hepatocellular carcinoma. *Cancer Science* **2009**, *100*, 1234–42.
(110) Petrocca, F.; Vecchione, A.; Croce, C. M. Emerging role of miR-106b-25/miR-17-92 clusters in the control of transforming growth factor beta signaling. *Cancer Research* **2008**, *68*, 8191–4.
(111) Poliseno, L.; Salmena, L.; Riccardi, L.; Fornari, A.; Song, S. M.; Hobbs, R. M.; Sportoletti, P.; Varmeh, S.; Egia, A.; Fedele, G.; Rameh, L.; Loda, M.; Pandolfi, P. P. Identification of the miR-106b~25 MicroRNA Cluster as a Proto- Oncogenic PTEN-Targeting Intron That Cooperates with Its Host Gene MCM7 in Transformation. *Science Signaling* **2010**, *3*, ra 29.
(112) Smith, A.; Iwanaga, R.; Drasin, D. J.; Micalizzi, D. S.; Vartuli, R. L.; Tan, A.-C.; Ford, H. L. The miR-106b-25 cluster targets Smad7, activates TGF-β signaling, and induces EMT and tumor initiating cell characteristics downstream of Six1 in human breast cancer. *Oncogene* **2012**, 1–10.
(113) Tanzer, A.; Stadler, P. F. Molecular evolution of a microRNA cluster. *Journal of Molecular biology* **2004**, *339*, 327–35.

(114) He, L.; Thomson, J. M.; Hemann, M. T.; Hernando-Monge, E.; Mu, D.; Goodson, S.; Powers, S.; Cordon-Cardo, C.; Lowe, S. W.; Hannon, G. J.; Hammond, S. M. A microRNA polycistron as a potential human oncogene. *Nature* **2005**, *435*, 828–833.
(115) Petrocca, F.; Visone, R.; Onelli, M. R.; Shah, M. H.; Nicoloso, M. S.; de Martino, I.; Iliopoulos, D.; Pilozzi, E.; Liu, C.-G.; Negrini, M.; Cavazzini, L.; Volinia, S.; Alder, H.; Ruco, L. P.; Baldassarre, G.; Croce, C. M.; Vecchione, A. E2F1-regulated microRNAs impair TGFbeta-dependent cell-cycle arrest and apoptosis in gastric cancer. *Cancer Cell* **2008**, *13*, 272–86.
(116) van den Brink, G. R.; Offerhaus, G. J. The morphogenetic code and colon cancer development. *Cancer Cell* **2007**, *11*, 109–17.
(117) Kan, T.; Sato, F.; Ito, T.; Matsumura, N.; David, S.; Agarwal, R.; Paun, B. C.; Jin, Z.; Olaru, A. V.; Florin, M.; Hamilton, J. P.; Yang, J.; Abraham, J. M.; Mori, Y.; Stephen, J. The miR-106b-25 polycistron, activated by genomic amplification, functions as an oncogene by suppressing p21 and Bim. *Gastroenterology* **2009**, *136*, 1689–1700.
(118) Cai, K.; Wang, Y.; Bao, X. MiR-106b promotes cell proliferation via targeting RB in laryngeal carcinoma. *Journal of Experimental & Clinical Cancer Research* **2011**, *30*, 73.
(119) Wang, H.; Liu, J.; Zong, Y.; Xu, Y.; Deng, W.; Zhu, H.; Liu, Y.; Ma, C.; Huang, L.; Zhang, L.; Qin, C. miR-106b aberrantly expressed in a double transgenic mouse model for Alzheimer's disease targets TGF-β type II receptor. *Brain Research* **2010**, *1357*, 166–74.
(120) Li, Z.; Yang, C.-S.; Nakashima, K.; Rana, T. M. Small RNA-mediated regulation of iPS cell generation. *The EMBO Journal* **2011**, *30*, 823–34.
(121) Debnath, J.; Muthuswamy, S. K.; Brugge, J. S. Morphogenesis and oncogenesis of MCF-10A mammary epithelial acini grown in three-dimensional basement membrane cultures. *Methods* **2003**, *30*, 256–268.
(122) Sambrook J, R. D. *Molecular Cloning: A Laboratory Manual*; 3rd ed.; Cold Spring Harbor Laboratory Press, 2001; p. 344.
(123) Bustin, S. a; Benes, V.; Garson, J. a; Hellemans, J.; Huggett, J.; Kubista, M.; Mueller, R.; Nolan, T.; Pfaffl, M. W.; Shipley, G. L.; Vandesompele, J.; Wittwer, C. T. The MIQE guidelines: minimum information for publication of quantitative real-time PCR experiments. *Clinical Chemistry* **2009**, *55*, 611–22.
(124) Fleige, S.; Walf, V.; Huch, S.; Prgomet, C.; Sehm, J.; Pfaffl, M. Comparison of relative mRNA quantification models and the impact of RNA integrity in quantitative real-time RT-PCR. *Biotechnology Letters* **2006**, *28*, 1601–1613.
(125) Vistica, D. T.; Skehan, P.; Scudiero, D.; Monks, A.; Pittman, A.; Boyd, M. R. Tetrazolium-based Assays for Cellular Viability : A Critical Examination of Selected Parameters Affecting Formazan Production. *Cancer Research* **1991**, *51*, 2515–2520.
(126) Rodriguez, L. G.; Wu, X.; Guan, J.-L. Wound-Healing Assay. *Methods in Molecular Biology* **2005**, *294*, 23–29.
(127) Saunders, M. Transplacental transport of nanomaterials. *Nanomedicine and Nanobiotechnology* **2009**, *1*, 671–84.

(128) Kleinman, H.; McGarvey, M.; Liotta, L.; Robey, P.; Tryggvason, K.; Martin, G. Isolation and characterization of type IV procollagen, laminin, and heparan sulfate proteoglycan from the EHS sarcoma. *Biochemistry* **1982**, *21*, 6188–6193.
(129) Albini, A.; Iwamoto, Y.; Kleinman, H. K.; Martin, G. R.; Aaronson, S. A.; Kozlowski, J. M.; Mcewan, R. N. A Rapid in Vitro Assay for Quantitating the Invasive Potential of Tumor Cells. *Cancer Research* **1987**, *47*, 3239–3245.
(130) Soule, H. D.; Maloney, T. M.; Wolman, S. R.; Peterson, W. D.; Brenz, R.; Mcgrath, C. M.; Russo, J.; Pauley, R. J.; Jones, R. F.; Brooks, S. C. Isolation and Characterization of a Spontaneously Immortalized Human Breast Epithelial Cell Line, MCF-10. *Cancer Research* **1990**, *50*, 6075–6086.
(131) Miletti-González, K. E.; Chen, S.; Muthukumaran, N.; Saglimbeni, G. N.; Wu, X.; Yang, J.; Apolito, K.; Shih, W. J.; Hait, W. N.; Rodríguez-Rodríguez, L. The CD44 receptor interacts with P-glycoprotein to promote cell migration and invasion in cancer. *Cancer Research* **2005**, *65*, 6660–7.
(132) Thangavel, C.; Boopathi, E.; Ertel, A.; Lim, M.; Addya, S.; Fortina, P.; Witkiewicz, Agnieszka K. Knudsen, E. S. Regulation of miR106b cluster through the RB pathway: Mechanism and functional targets. *Cell Cycle* **2013**, *12*, 98–111.
(133) Fang, L.; Deng, Z.; Shatseva, T.; Yang, J.; Peng, C.; Du, W. W.; Yee, a J.; Ang, L. C.; He, C.; Shan, S. W.; Yang, B. B. MicroRNA miR-93 promotes tumor growth and angiogenesis by targeting integrin-β8. *Oncogene* **2011**, *30*, 806–21.
(134) Friedl, P.; Alexander, S. Cancer invasion and the microenvironment: plasticity and reciprocity. *Cell* **2011**, *147*, 992–1009.
(135) Karlin, J. D.; Nguyen, D.; Yang, S. X.; Lipkowitz, S. Epidermal growth factor receptor expression in breast cancer. *Journal of Clinical Oncology* **2005**, *23*, 8118–8141.
(136) Hou, Y.; Hedberg, S.; Schneider, I. C. Differences in adhesion and protrusion properties correlate with differences in migration speed under EGF stimulation. *BMC Biophysics* **2012**, *5*, 8.
(137) Park, J. H.; Han, H. J. Caveolin-1 plays important role in EGF-induced migration and proliferation of mouse embryonic stem cells: involvement of PI3K/Akt and ERK. *American Journal of Physiology. Cell Physiology* **2009**, *297*, C935–44.
(138) Andl, C. D.; Mizushima, T.; Oyama, K.; Bowser, M.; Nakagawa, H.; Rustgi, A. K. EGFR-induced cell migration is mediated predominantly by the JAK-STAT pathway in primary esophageal keratinocytes. *American Journal of Physiology. Gastrointestinal and Liver Physiology* **2004**, *287*, G1227–37.
(139) Katz, M.; Amit, I.; Citri, A.; Shay, T.; Carvalho, S.; Lavi, S.; Milanezi, F.; Lyass, L.; Amariglio, N.; Jacob-Hirsch, J.; Ben-Chetrit, N.; Tarcic, G.; Lindzen, M.; Avraham, R.; Liao, Y.-C.; Trusk, P.; Lyass, A.; Rechavi, G.; Spector, N. L.; Lo, S. H.; Schmitt, F.; Bacus, S. S.; Yarden, Y. A reciprocal tensin-3-cten switch mediates EGF-driven mammary cell migration. *Nature Cell Biology* **2007**, *9*, 961–9.

(140) Ridley, A. J.; Schwartz, M. a; Burridge, K.; Firtel, R. a; Ginsberg, M. H.; Borisy, G.; Parsons, J. T.; Horwitz, A. R. Cell migration: integrating signals from front to back. *Science* **2003**, *302*, 1704–9.
(141) Irie, H. Y.; Pearline, R. V.; Grueneberg, D.; Hsia, M.; Ravichandran, P.; Kothari, N.; Natesan, S.; Brugge, J. S. Distinct roles of Akt1 and Akt2 in regulating cell migration and epithelial-mesenchymal transition. *The Journal of Cell Biology* **2005**, *171*, 1023–34.
(142) Chen, H.; Lo, S. H. Regulation of tensin-promoted cell migration by its focal adhesion binding and Src homology domain 2. *Biochemical Journal* **2003**, *370*, 1039–1045.
(143) Henson, E. S.; Gibson, S. B. Surviving cell death through epidermal growth factor (EGF) signal transduction pathways: Implications for cancer therapy. *Cellular Signaling* **2006**, *18*, 2089–2097.
(144) Normanno, N.; De Luca, A.; Bianco, C.; Strizzi, L.; Mancino, M.; Maiello, M. R.; Carotenuto, A.; De Feo, G.; Caponigro, F.; Salomon, D. S. Epidermal growth factor receptor (EGFR) signaling in cancer. *Gene* **2006**, *366*, 2–16.
(145) Levy, D. E.; Darnell, J. E. STATs: transcriptional control and biological impact. *Nature Reviews. Molecular Cell Biology* **2002**, *3*, 651–662.
(146) Wang, Y.; Wang, X.; Zhang, J.; Sun, G.; Luo, H.; Kang, C.; Pu, P.; Jiang, T.; Liu, N.; You, Y. MicroRNAs involved in the EGFR/PTEN/AKT pathway in gliomas. *Journal of Neuro-oncology* **2012**, *106*, 217–24.
(147) Neve, R. M.; Chin, K.; Fridlyand, J.; Yeh, J.; Baehner, F. L.; Fevr, T.; Clark, L.; Bayani, N.; Coppe, J.-P.; Tong, F.; Speed, T.; Spellman, P. T.; DeVries, S.; Lapuk, A.; Wang, N. J.; Kuo, W.-L.; Stilwell, J. L.; Pinkel, D.; Albertson, D. G.; Waldman, F. M.; McCormick, F.; Dickson, R. B.; Johnson, M. D.; Lippman, M.; Ethier, S.; Gazdar, A.; Gray, J. W. A collection of breast cancer cell lines for the study of functionally distinct cancer subtypes. *Cancer Cell* **2006**, *10*, 515–527.
(148) Pishvaian, M. J.; Feltes, C. M.; Thompson, P.; Bussemakers, M. J.; Schalken, J. A.; Byers, S. W. Cadherin-11 Is Expressed in Invasive Breast Cancer Cell Lines. *Cancer Research* **1999**, *59*, 947–952.
(149) Collagenase, I. V.; Ht, F.; Devarajans, P.; Johnston, J. J.; Ginsberg, S. S.; Wartqli, H. E. V. Structure and Expression of Neutrophil Gelatinase cDNA. *The Journal of Biological Chemistry* **1992**, *267*, 25228–25232.
(150) Llano, E.; Pendás, A. M.; Freije, J. P.; Penda, A. M.; Murphy, G.; Lo, C. Identification and Characterization of Human MT5-MMP , a New Membrane-bound Activator of Progelatinase A Overexpressed in Brain Tumors. *Cancer Research* **1999**, *59*, 2570–2576.

APPENDIX A

VECTOR

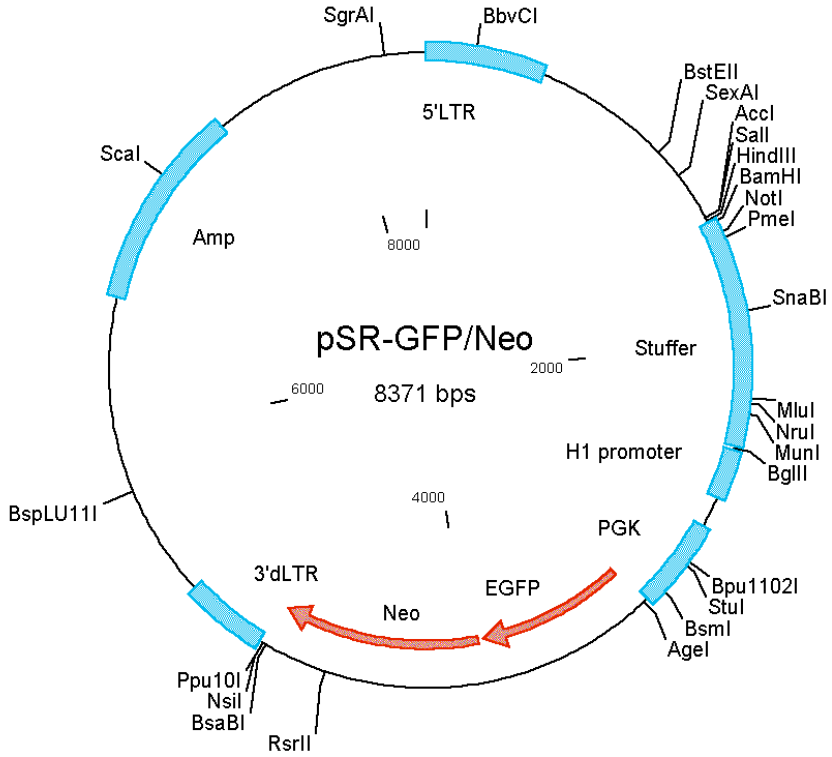

Figure A. Map of pSUPER.retro.neo+GFP (Invitrogen).

APPENDIX B

TESTING SUCCESS of DNase TREATMENT

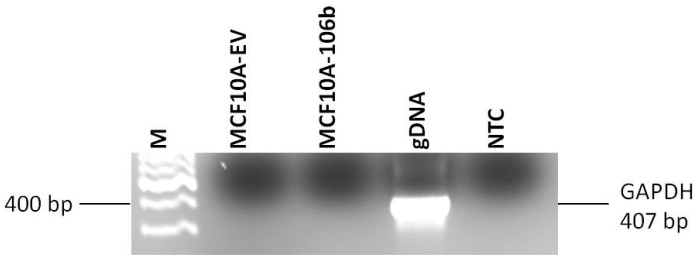

Figure B. Lack of DNA contamination in RNA samples after DNase treatment was assessed via PCR using GAPDH specific primers (sequences in Table 2.3). Cycling conditions are stated in Table 2.5. Observing no bands in MCF10A-EV and MCF10A-106b confirms the success of DNase treatment.

APPENDIX C

MIQE GUIDELINES

Table C. MIQE Guidelines Checklist for qRT-PCR

ITEM TO CHECK	IMPORTANCE	CHECKLIST	COMMENTS/WHERE
EXPERIMENTAL DESIGN			
Definition of experimental and control groups	**E**	**YES**	Materials and Methods
Number within each group	**E**	**YES**	Materials and Methods
Assay carried out by core lab or investigator's lab?	D	**YES**	Investigator's Lab
Acknowledgement of authors' contributions	D	**NO**	
SAMPLE			
Description	**E**	**N/A**	
Volume/mass of sample processed	D	**N/A**	
Microdissection or macrodissection	**E**	**N/A**	
Processing procedure	**E**	**N/A**	
If frozen - how and how quickly?	**E**	**N/A**	
If fixed - with what, how quickly?	**E**	**N/A**	
Sample storage conditions and duration (especially for FFPE samples)	**E**	**N/A**	
NUCLEIC ACID EXTRACTION			
Procedure and/or instrumentation	**E**	**YES**	Materials and Methods (page 20)
Name of kit and details of any modifications	**E**	**YES**	Materials and Methods (page 20)
Source of additional reagents used	D	**YES**	Materials and Methods (page 20)
Details of DNase or RNAse treatment	**E**	**N/A**	Not required in TaqMan assay
Contamination assessment (DNA or RNA)	**E**	**N/A**	Not required in TaqMan assay
Nucleic acid quantification	**E**	**YES**	Materials and Methods (page 20)
Instrument and method	**E**	**YES**	Materials and Methods (page 20)
Purity (A260/A280)	**E**	**YES**	Fig. C1.
Yield	D	**YES**	Fig. C1.
RNA integrity method/instrument	**E**	**NO**	
RIN/RQI or Cq of 3' and 5' transcripts	**E**	**NO**	
Electrophoresis traces	D	**N/A**	
Inhibition testing (Cq dilutions, spike or other)	**E**	**YES**	Cq dilutions Fig. C2, Fig. C3.
REVERSE TRANSCRIPTION			
Complete reaction conditions	**E**	**YES**	Materials and methods (page 21)
Amount of RNA and reaction volume	**E**	**YES**	Materials and methods (page 21)
Priming oligonucleotide and concentration	**E**	**NO**	Manufactures proprietary
Reverse transcriptase and concentration	**E**	**YES**	Materials and methods (page 21)
Temperature and time	**E**	**YES**	Materials and methods (page 21)
Manufacturer of reagents	D	**YES**	Materials and methods (page 21)
Cqs with and without RT	D	**NO**	
Storage conditions of cDNA	D	**YES**	Materials and methods (page 21)

Table C. Continued. MIQE Guidelines Checklist for qRT-PCR

qPCR TARGET INFORMATION			
If multiplex, efficiency and LOD of each assay	**E**	**N/A**	
Sequence accession number	**E**	**YES**	hsa-miR-106b: NR_029831.1 RNU6B: NR_002752
Location of amplicon	D	**NO**	Manufactures proprietary
Amplicon length	**E**	**NO**	Manufactures proprietary
In silico specificity screen (BLAST, etc)	**E**	**NO**	Manufactures proprietary
Pseudogenes, retropseudogenes or other homologs?	D	**NO**	Manufactures proprietary
Sequence alignment	D	**NO**	Manufactures proprietary
Secondary structure analysis of amplicon	D	**NO**	Manufactures proprietary
Location of each primer by exon or intron (if applicable)	**E**	**NO**	Manufactures proprietary
What splice variants are targeted?	**E**	**NO**	Manufactures proprietary
qPCR OLIGONUCLEOTIDES			
Primer sequences	**E**	**NO**	Manufactures proprietary
RTPrimerDB Identification Number	D	**N/A**	
Probe sequences	D	**NO**	Manufactures proprietary
Location and identity of any modifications	**E**	**NO**	Manufactures proprietary
Manufacturer of oligonucleotides	D	**YES**	Materials and Methods (page 23)
Purification method	D	**NO**	Manufactures proprietary
qPCR PROTOCOL			
Complete reaction conditions	**E**	**YES**	Materials and methods (page 24)
Reaction volume and amount of cDNA/DNA	**E**	**YES**	Materials and methods (page 24)
Primer, (probe), Mg++ and dNTP concentrations	**E**	**NO**	Manufactures proprietary
Polymerase identity and concentration	**E**	**NO**	Manufactures proprietary
Buffer/kit identity and manufacturer	**E**	**YES**	Materials and methods (page 24)
Exact chemical constitution of the buffer	D	**NO**	Manufactures proprietary
Additives (SYBR Green I, DMSO, etc.)	**E**	**N/A**	
Manufacturer of plates/tubes and catalog number	D	**YES**	
Complete thermocycling parameters	**E**	**YES**	Materials and methods (page 24)
Reaction setup (manual/robotic)	D	**YES**	Manual setup
Manufacturer of qPCR instrument	**E**	**YES**	Materials and methods (page 24)
qPCR VALIDATION			
Evidence of optimization (from gradients)	D	**NO**	
Specificity (gel, sequence, melt, or digest)	**E**	**N/A**	
Cq of the NTC	**E**	**YES**	Fig. C2, Fig. C3
Standard curves with slope and y-intercept	**E**	**YES**	Fig. C2, Fig. C3
PCR efficiency calculated from slope	**E**	**YES**	Fig. C2, Fig. C3
Confidence interval for PCR efficiency or standard error	D	**N/A**	
r2 of standard curve	**E**	**YES**	Fig. C2, Fig. C3
Linear dynamic range	**E**	**YES**	Fig. C2, Fig. C3
Cq variation at lower limit	**E**	**YES**	Fig. C2, Fig. C3
Confidence intervals throughout range	D	**N/A**	
Evidence for limit of detection	**E**	**NO**	

Table C.Continued. MIQE Guidelines Checklist for qRT-PCR

If multiplex, efficiency and LOD of each assay	**E**	**N/A**	
DATA ANALYSIS			
qPCR analysis program (source, version)	**E**	**YES**	Materials and methods (page 26)
Cq method determination	**E**	**YES**	Materials and methods (page 26)
Outlier identification and disposition	**E**	**N/A**	
Results of NTCs	**E**	**YES**	Fig. C2, Fig. C3
Justification of number and choice of reference genes	**E**	**NO**	Manufactures proprietary
Description of normalization method	**E**	**YES**	Standard curve method
Number and concordance of biological replicates	D	**YES**	Materials and methods (page 26)
Number and stage (RT or qPCR) of technical replicates	**E**	**YES**	Materials and methods (page 26)
Repeatability (intra-assay variation)	**E**	**YES**	Materials and methods (page 26)
Reproducibility (inter-assay variation, %CV)	D	**N/A**	
Power analysis	D	**NO**	
Statistical methods for result significance	**E**	**YES**	Biological replicates
Software (source, version)	**E**	**YES**	Materials and methods (page 26)
Cq or raw data submission using RDML	D	**N/A**	

E: Essential, D: Desirable, N/A: Not Applicable

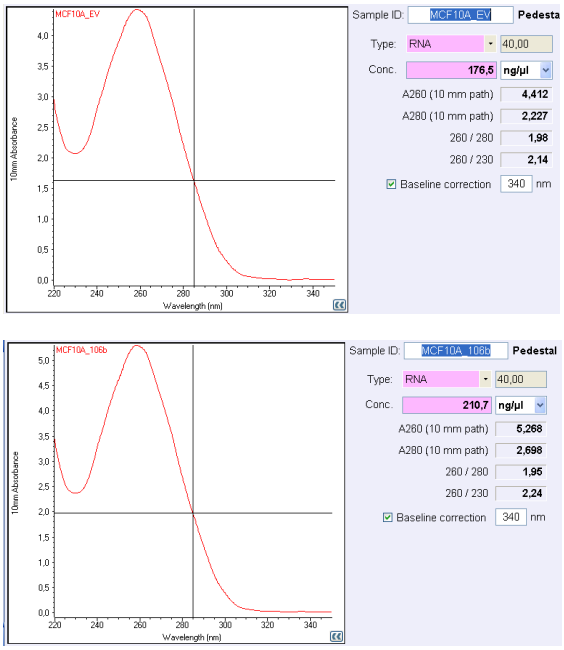

Figure C1. RNA concentrations (A_{260}) of MCF10A-EV and MCF10A-106b. Concentrations were measured by using NanoDrop ND1000 (Thermo Scientific). Purity of samples was assessed by A_{260} /A_{280} and A_{260} /A_{230} ratios (RNA samples were around 2.0 for A_{260} /A_{280} and A_{260} /A_{230} ratios).

Raw Data For Cycling A.Green

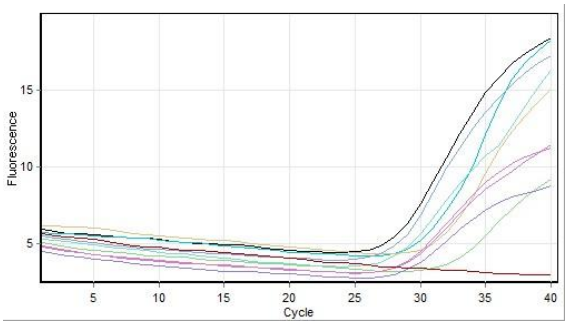

Quantitation data for Cycling A.Green

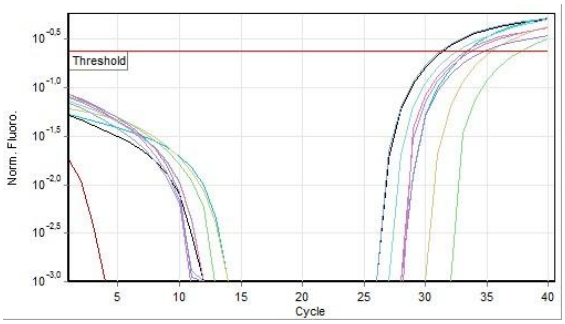

Standard Curve

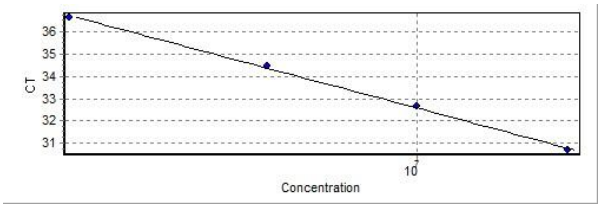

No.	Colour	Name	Type	Ct	Given Conc (Copies)	Calc Conc (Copies)	% Var
1		Std-1 RNU6B	Standard	30,69	20.000.000	20.715.715	3,6%
2		Std-2 RNU6B	Standard	32,64	10.000.000	9.730.516	2,7%
3		Std-3 RNU6B	Standard	34,46	5.000.000	4.802.159	4,0%
4		Std-4 RNU6B	Standard	36,63	2.000.000	2.066.130	3,3%
5		ntc u6	NTC				

Figure C2. qRT-PCR assay performance shown with respect to MIQE guidelines. Raw fluoresence data, quantitation data, standard curve and quantitation information was analyzed by RotorGene Software for RNU6B primers. In TaqMan probe systems melting curve analysis is not performed.

Quantitation Information

Threshold	0,2396
Left Threshold	1,000
Standard Curve Imported	No
Standard Curve (1)	conc= 10^(-0,169*CT + 12,490)
Standard Curve (2)	CT = -5,933*log(conc) + 74,101
Reaction efficiency (*)	0,47417 (* = 10^(-1/m) - 1)
M	-5,93299
B	74,10149
R Value	0,9992
R^2 Value	0,99839
Start normalising from cycle	18
Noise Slope Correction	No
No Template Control Threshold	0%
Reaction Efficiency Threshold	Disabled
Normalisation Method	Dynamic Tube Normalisation
Digital Filter	Light
Sample Page	Page 1
Imported Analysis Settings	

Figure C2. Continued. qRT-PCR assay performance shown with respect to MIQE guidelines. Raw fluoresence data, quantitation data, standard curve and quantitation information was analyzed by RotorGene Software for RNU6B primers. In TaqMan probe systems melting curve analysis is not performed.

Raw Data For Cycling A.Green

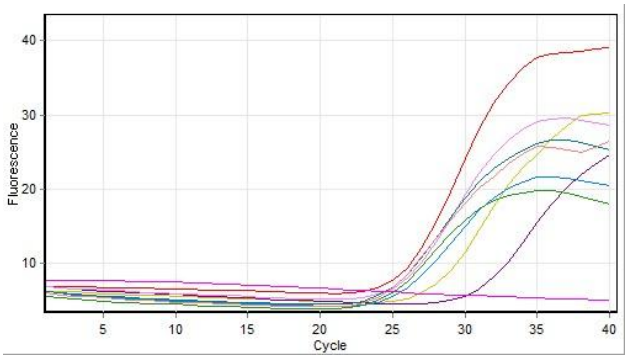

Quantitation data for Cycling A.Green

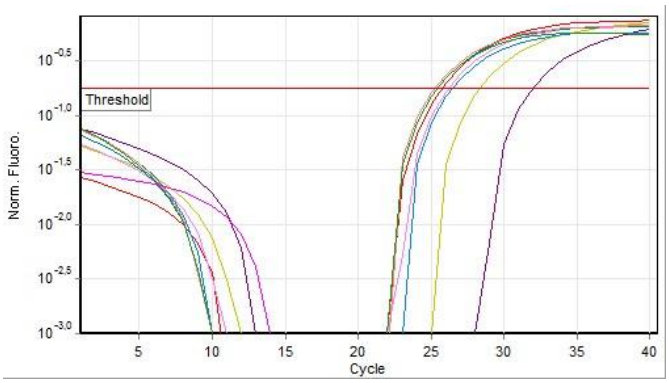

Standard Curve

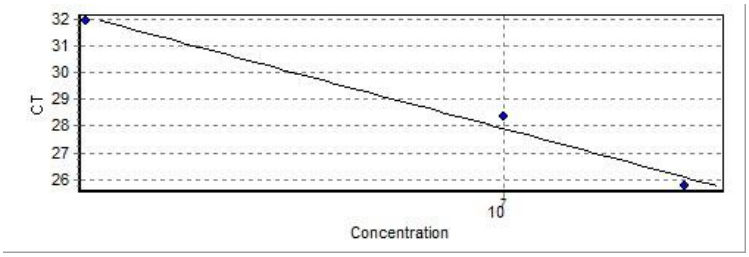

No.	Colour	Name	Type	Ct	Given Conc (Copies)	Calc Conc (Copies)	% Var
1		Std-1 miR-106b	Standard	25,75	20.000.000	22.711.782	13,6%
2		Std-2 miR-106b	Standard	28,37	10.000.000	8.336.741	16,6%
3		Std-3 miR-106b	Standard	31,97	2.000.000	2.112.577	5,6%
4		ntc miR-106	NTC				

Figure C3. qRT-PCR assay performance shown with respect to MIQE guidelines. Raw fluoresence data, quantitation data, standard curve and quantitation information was analyzed by RotorGene Software for miR-106b primers. In TaqMan probe systems melting curve analysis is not performed.

Quantitation Information

Threshold	0,1784
Left Threshold	1,000
Standard Curve Imported	No
Standard Curve (1)	conc= 10^(-0,166*CT + 11,630)
Standard Curve (2)	CT = -6,025*log(conc) + 70,075
Reaction efficiency (*)	0,46544 (* = 10^(-1/m) - 1)
M	-6,0252
B	70,07527
R Value	0,99077
R^2 Value	0,98162
Start normalising from cycle	1
Noise Slope Correction	No
No Template Control Threshold	0%
Reaction Efficiency Threshold	Disabled
Normalisation Method	Dynamic Tube Normalisation
Digital Filter	Light
Sample Page	Page 1
Imported Analysis Settings	

Figure C3. Continued. qRT-PCR assay performance shown with respect to MIQE guidelines. Raw fluoresence data, quantitation data, standard curve and quantitation information was analyzed by RotorGene Software for miR-106b primers. In TaqMan probe systems melting curve analysis is not performed.